Neurobiology of Stress 13 (2020) 100267

Contents lists available at ScienceDirect

Neurobiology of Stress

journal homepage: www.elsevier.com/locate/ynstr

Early life stress dysregulates kappa opioid receptor signaling within the lateral habenula

Sarah C. Simmons, Ryan D. Shepard, Shawn Gouty, Ludovic D. Langlois, William J. Flerlage, Brian M. Cox, Fereshteh S. Nugent *

Uniformed Services University of the Health Sciences, Edward Hebert School of Medicine, Department of Pharmacology and Molecular Therapeutics, Bethesda, MD, 20814, USA

ARTICLE INFO

Keywords:
Lateral habenula
LHb
Kappa opioid receptor
KOR
Dynorphin
Early life stress

ABSTRACT

The lateral habenula (LHb) is an epithalamic brain region associated with value-based decision making and stress evasion through its modulation of dopamine (DA)-mediated reward circuitry. Specifically, increased activity of the LHb is associated with drug addiction, schizophrenia and stress-related disorders such as depression, anxiety and posttraumatic stress disorder. Dynorphin (Dyn)/Kappa opioid receptor (KOR) signaling is a mediator of stress response in reward circuitry. Previously, we have shown that maternal deprivation (MD), a severe early life stress, increases LHb spontaneous neuronal activity and intrinsic excitability while blunting the response of LHb neurons to extrahypothalamic corticotropin-releasing factor (CRF) signaling, another stress mediator. CRF pathways also interact with Dyn/KOR signaling. Surprisingly, there has been little study of direct KOR regulation of the LHb despite its distinct role in stress, reward and aversion processing. To test the functional role of Dyn/KOR signaling in the LHb, we utilized ex-vivo electrophysiology combined with pharmacological tools in rat LHb slices. We show that activation of KORs by a KOR agonist (U50,488) exerted differential effects on the excitability of two distinct sub-populations of LHb neurons that differed in their expression of hyperpolarization-activated cation currents (HCN, Ih). Specifically, KOR stimulation increased neuronal excitability in LHb neurons with large Ih currents (Ih+) while decreasing neuronal excitability in small/negative Ih (Ih-) neurons. We found that an intact fast-synaptic transmission was required for the effects of U50,488 on the excitability of both Ih- and Ih+ LHb neuronal subpopulations. While AMPAR-, $GABA_AR$-, or NMDAR-mediated synaptic transmission alone was sufficient to mediate the effects of U50,488 on excitability of Ih- neurons, either $GABA_AR$- or NMDAR-mediated synaptic transmission could mediate these effects in Ih+ neurons. Consistently, KOR activation also altered both glutamatergic and GABAergic synaptic transmission where stimulation of presynaptic KORs uniformly suppressed glutamate release onto LHb neurons while primarily decreased or in some cases increased GABA release. We also found that MD significantly increased immunolabeled Dyn (the endogenous KOR agonist) labeling in neuronal fibers in LHb while significantly decreasing mRNA levels of KORs in LHb tissues compared to those from non-maternally deprived (non-MD) control rats. Moreover, the U50,488-mediated increase in LHb neuronal firing observed in non-MD rats was absent following MD. Altogether, this is the first demonstration of the existence of functional Dyn/KOR signaling in the LHb that can be modulated in response to severe early life stressors such as MD.

Abbreviations: action potential, (AP); adverse childhood experiences, (ACE); artificial cerebral spinal fluid, (ACSF); corticotropin-releasing factor, (CRF); dopamine, (DA); dynorphin, (Dyn); early life stress, (ELS); fastafterhyperpolarization, (fAHP); hyperpolarization activated cation current, (HCN, Ih); input resistance, (Rin); inter-event interval, (IEI); Kappa opioid receptor, (KOR); maternal deprivation, (MD); medium afterhyperpolarization, (mAHP); miniature excitatory postsynaptic current, (mEPSC); miniature inhibitory postsynaptic current, (mIPSC); non-maternally deprived, (non-MD); nucleus accumbens, (NAc); postnatal age, (PN); raphe nuclei, (RN); rostromedial tegmental area, (RMTg); serotonin, (5HT); ventral tegmental area, (VTA).

* Corresponding author.
E-mail address: fereshteh.nugent@usuhs.edu (F.S. Nugent).

https://doi.org/10.1016/j.ynstr.2020.100267
Received 14 July 2020; Received in revised form 16 October 2020; Accepted 9 November 2020
Available online 17 November 2020

1. Introduction

Depression is a major health concern in the United States with a prevalence of 7% of all adults or 13% of all adolescents (age12-17) in 2017 (S.A.a.M.H.S. Administration., 2019; S.A.a.M.H.S. Administration et al., 2017). Those who experience severe early life stress (ELS) or adverse childhood events (ACE) have increased risk for the development of depression, suicidal ideation and suicide attempts later in life (Jones et al., 2020; Chapman et al., 2004; Heim and Nemeroff, 2001; Thompson et al., 2019). 61% of the US population have experienced at least 1 ACE, and 16% have experienced 4 or more, putting a significant population at increased risk for developing mood-disorders later in life (Jones et al., 2020). In order to better understand the interaction of ELS/ACE and increased susceptibility to development of a mood-disorder (such as anxiety or depression) we use a preclinical rodent model of severe childhood neglect - maternal deprivation (MD). In this model, neonatal rat pups are separated from the dam for a single 24hr period which induces long-lasting effects on depressive-like behavior that can be reversed by common antidepressant treatments effective in treating depression in human subjects (Shepard, 2018a, 2020; Authement et al., 2015; Faturi et al., 2010; Llorente et al., 2010). Additionally, we have found that MD alters the activity of key reward/aversion processing regions such as the ventral tegmental area (VTA) and the lateral habenula (LHb) (Shepard et al., 2018a, 2018b, 2020; Authement et al., 2015, 2018). The LHb is an epithalamic brain region that is now recognized as an emerging anti-reward hub implicated in motivation and decision-making. Neuronal pathways through LHb link forebrain limbic structures with midbrain monoaminergic centers (Stamatakis and Stuber, 2012; Proulx et al., 2014, 2018; Hu et al., 2020; Hikosaka, 2010). LHb is involved in reward/aversion-related learning and memory processes associated with avoidance from stressful and aversive situations through suppression of dopamine (DA) and serotonin (5HT) systems and its increased activity is associated with depression in human studies and depression-like phenotypes across a variety of animal models of stress (Shepard et al., 2018a; Authement et al., 2018; Cerniauskas et al., 2019; Berger et al., 2018; Nuno-Perez et al., 2018; Yang et al., 2018a, 2018b; Tchenio et al., 2017).

The dynorphin-Kappa opioid receptor (Dyn/KOR) system is highly implicated in regulating states of motivation and emotion, and in the development of mood disorders, including depression and anxiety, as well as in drug addiction and stress-induced relapse to drug-taking (Margolis and Karkhanis, 2019; Tejeda and Bonci, 2019; Bruchas et al., 2010; Karkhanis et al., 2016; Carr et al., 2010; Van Bockstaele et al., 2010). Activation of Dyn/KOR signaling in response to acute stress increases motivation to escape an immediate threat, whereas prolonged activation of this signaling during chronic stress leads to dysregulation of this neuromodulatory system by producing aversion that counteracts positive reinforcement and contributes to the development of pro-depressive, anti-social and negative affective and emotional states associated with mood/stress-related disorders as well as addiction (Bruchas et al., 2010). While there is evidence for direct Dyn/KOR regulation of the mesocorticolimbic system (Margolis and Karkhanis, 2019; Abraham et al., 2018; Ehrich et al., 2015; Ford et al., 2007), to date there has been little study of KOR regulation of other important stress/mood-related regions such as the LHb. Dyn/KORs are abundant in reward and aversion brain structures projecting to the LHb. For example, the LHb receives significant inputs from pro-dynorphin expressing brain regions with high levels of KOR expression such as lateral hypothalamus, amygdala, nucleus accumbens (NAc), dorsal striatum, and globus pallidus internal (also referred to as the entopeduncular nucleus in rodents) (Yang et al., 2018b; Tejeda and Bonci, 2019; Crowley et al., 2016; Zamir et al., 1984; Code and Fallon, 1986; Vincent et al., 1982; Cahill et al., 2014). KOR expression has also been reported in the LHb in addition to mu opioid receptors (MOR) and delta opioid receptors (DOR) (Mansour et al., 1987; Chen et al., 2020), also raising the possibility of postsynaptic modulation of LHb neurons by Dyn/KOR signaling in addition to presynaptic effects through inputs projecting to the LHb. Therefore, the LHb is poised to be not only a potent regulator of affective disorders and addiction, but also a possible hotspot for Dyn/KOR regulation of motivation, stress and mood.

Here we first established the role of Dyn/KOR signaling in modulating LHb activity through both intrinsic properties and synaptic modulation. We provide significant evidence for the presence of a functional Dyn/KOR signaling in the LHb that individually alters the activity of two discrete populations of LHb neurons discriminated by the presence or absence of hyperpolarization-activated cation currents (HCN, Ih). Additionally, we found that KOR activation in LHb directly modulated glutamatergic and GABAergic synaptic transmission in the LHb, contributing to changes in overall LHb excitability. Secondly, we assessed whether this Dyn/KOR regulation of LHb neuronal excitability was altered following MD. We found that MD dysregulated Dyn/KOR signaling, resulting in a loss of acute KOR modulation of LHb neuronal excitability. To our knowledge, this is the first study directly assessing the effects of Dyn/KOR signaling in the LHb, and providing evidence for Dyn/KOR dysregulation in the LHb following a severe ELS.

2. Methods

2.1. Animals

All experiments employed male Sprague Dawley rats (sourced from Taconics Inc., and Charles River) in experiments conducted in accordance with the National Institutes of Health Guide for the Care and Use of Laboratory Animals and were approved by the Uniformed Services University Institutional Animal Care and Use Committee. All rats were received on post-natal day 6 (PN6) with lactating dam and allowed to acclimate undisturbed for ~72hr before initiation of the MD procedure. All rats were kept on a 12hr dark: 12hr light cycle schedule with lights on at 06:00, and all procedures began 3–4 h after the start of the light-cycle. All animals received ad-lib standard chow and water (except where noted during the MD procedure). All efforts were made to minimize animal suffering and reduce the number of animals used throughout this study.

2.2. MD procedure

MD was performed on male rats at PN9. Half of a litter (randomly selected) were isolated from the dam and their siblings for 24hrs (MD group). The isolated pups were placed on a heating pad (34°C) in a separate quiet room and not disturbed for 24hr until being returned to their home cage. The remaining non-MD control group received the same amount of handling. For electrophysiology, and qPCR experiments all rat pups were sacrificed during the adolescent age range of PN21-PN28. For IHC experiments, rats were sacrificed at ages PN16 (young), PN28 (adolescent), and PN60 (adult). For IHC of adult animals, all rats were co-housed (2 per cage, treatment matched) from weaning at PN28 to sacrifice at PN60 and received standard housing care but no additional experimenter manipulation prior to sacrifice.

2.3. Slice preparation

For all electrophysiology experiments several separate cohorts of non-MD/MD treated rats were used. As described before (Authement et al., 2018) all rats were anesthetized with isoflurane, decapitated and brains were quickly dissected and placed into ice-cold artificial cerebrospinal fluid (ACSF) containing (in mM): 126 NaCl, 21.4 NaHCO3, 2.5 KCl, 1.2 NaH2PO4, 2.4 CaCl2, 1.00 MgSO4, 11.1 glucose, 0.4 mM ascorbic acid and saturated with 95% O_2-5% CO_2. Briefly, sagittal slices containing LHb were cut at 250 μm and incubated in above prepared ACSF at 34 °C for at least 1hr prior to electrophysiological experiments. For patch clamp recordings, slices were then transferred to a recording chamber and perfused with ascorbic-acid free ACSF at 28 °C.

2.4. Electrophysiology

Voltage-clamp cell-attached and whole-cell voltage/current-clamp recordings were performed from LHb neurons in LHb-containing slices using patch pipettes (3–6 MOhms, MΩ) and a patch amplifier (MultiClamp 700B) under infrared-differential interference contrast microscopy. Data acquisition and analysis were carried out using DigiData 1440A, pCLAMP 10 (Molecular Devices), Clampfit, and Mini Analysis 6.0.3 (Synaptosoft Inc.). Signals were filtered at 3 kHz and digitized at 10 kHz.

To assess LHb spontaneous activity, LHb neuronal activity/excitability and intrinsic membrane properties in intact synaptic transmission, cells were patch clamped with potassium-gluconate based internal solution (130 mM K-gluconate, 15 mM KCl, 4 mM adenosine triphosphate (ATP)–Na+, 0.3 mM guanosine triphosphate (GTP)–Na+, 1 mM EGTA, and 5 mM Hepes, pH adjusted to 7.28 with KOH, osmolarity adjusted to 275–280 mOsm) in slices perfused with ACSF. In a separate set of experiments, intrinsic neuronal excitability experiments were performed in the absence of fast-synaptic transmission by addition of AMPAR antagonist 6,7 dinitroquinoxaline-2,3-dione di-sodium salt (DNQX, 10 μM,Tocris-2312), $GABA_AR$ antagonist picrotoxin (PTX, 100 μM, Tocris-1128), and NMDAR antagonist D-(-)-2-Amino-5- phosphonopentanoic acid (APV, 50 μM, Tocris-0106) to the ACSF. Additional separate experiments were performed in the presence of a single synaptic receptor blocker (DNQX, APV, or PTX) similar to previous experiments. Across all experiments, spontaneous neuronal activity and AP firing patterns (tonic, bursting) were assessed in both cell-attached recordings in voltage-clamp mode at V = 0 mV and whole cell recording in current-clamp mode at I = 0 pA for the duration of ~1min recording. Cells that fired less than 2 action potentials (AP) during this time period were characterized as silent. Resting membrane potential (RMP) was assessed immediately after achieving whole-cell patch configuration in current clamp recordings. Ih current recordings were performed in voltage-clamp in response to stepping cells from −50 mV to −100 mV (700 ms duration). Ih positive (Ih+) neurons were defined as having a maximal Ih current (peak to steady state trough) response >−10 pA (and conversely Ih- neurons as ≤ −10 pA).

During LHb neuronal excitability recordings in current-clamp mode, AP generation was assessed in response to increasingly depolarizing current steps ranging from +10 to +100 pA (+10 pA ea. step) while cells were kept at −67 to −70mV with manual direct current injection between pulses. Current steps were 5s in duration with 25s inter-stimulus intervals. The number of APs induced by depolarization at each intensity was counted and averaged for each experimental group at each step. Input resistance (Rin) was measured at −50pA step (5s duration) and calculated by dividing the change in voltage response by the current-pulse amplitude and presented as MΩ. AP number, AP threshold, fast after-hyperpolarizations (fAHP), medium after-hyperpolarizations (mAHP), AP half-width, AP amplitude were assessed using clampfit and measured from the first AP at the current step that was sufficient to generate the first AP/s as previously described (Authement et al., 2018).

Whole cell recordings of AMPAR-meditated miniature excitatory postsynaptic currents (mEPSC) were performed in ACSF perfused with PTX (100 μM), APV (50 μM), and tetrodotoxin (TTX, 1 μM). Patch pipettes for mEPSCs recordings were filled with cesium (Cs)-gluconate internal solution (117 mM Cs-gluconate, 2.8 mM NaCl, 5 mM $MgCl_2$, 2 mM ATP-Na+, 0.3 mM GTP-Na+, 0.6 mM EGTA, and 20 mM Hepes, pH adjusted to 7.28 using CsOH, osmolarity adjusted to 275–280 mOsm). Whole-cell recordings of $GABA_AR$-mediated miniature inhibitory postsynaptic currents (mIPSC) were performed in ACSF perfused with APV (50 μM), DNQX (10 μM), glycine receptor inhibitor (strychnine, 1 μM), and TTX, 1 μM. Patch pipettes were filled with KCl internal solution (125 mM KCl, 2.8 mM NaCl, 2 mM $MgCl_2$, 2 mM ATP Na+, 0.3 mM GTP-Na+, 0.6 mM EGTA, and 10 mM Hepes, pH adjusted to 7.28 with KOH, osmolarity adjusted to 275–280mOsm). For both mEPSCs and mIPSCs, LHb neurons were voltage-clamped at −70mV and recorded over 10 sweeps, each lasting 50s. The cell series resistance was monitored through all the experiments and if this value changed by more than 10%, data were not included.

2.5. Drugs

For all agonist/antagonist experiments a within-subjects experimental design was used. Baseline recordings were first performed (depolarization-induced AP recordings/mEPSC/mIPSC) for each neuron and then appropriate drug was added to the slice by the perfusate and responses tested following 30–45min of drug bath application. In all experiments stimulating KORs, the KOR agonist (+/-)U50,488 (Tocris, 10 μM) was used. To test specificity of U50,488 effects, we used a novel selective KOR antagonist (BTRX-084266, 10–20 μM) generously provided by BlackThorn, Inc. We also validated these results with KOR-antagonist aticaprant (also known as Cerc501; 1–5 μM). LHb-containing slices were incubated with BTRX-084266 for at least 30min prior to U50,488 application. Aticaprant was applied through bath application for at least 10–30min before experiment start.

2.6. Immunohistochemistry and image analyses

Rats were anesthetized with an intraperitoneal injection containing ketamine (85 mg/kg) and xylazine (10 mg/kg) and perfused through the aorta with 1x phosphate buffered saline (PBS), followed by 4% paraformaldehyde (PFA) (Santa Cruz). Juvenile, adolescent or adult rats (PN16, PN21-28 or PN60) were perfused similarly but with adjusted volumes of between 200 and 250 ml each solution. The brains were dissected and placed in 4% PFA for 24 h and then cryoprotected by submersion in 20% sucrose for 3 days, frozen on dry ice, and stored at −70°C until sectioned. Sections of the LHb were cut using a cryostat (Leica CM1900) and mounted on slides. Serial coronal sections (20 mμ) of the midbrain containing the LHb (from −2.64 to −4.36 mm caudal to bregma (Paxinos and Watson, 2007) were briefly fixed in 4% PFA for 5 min, washed in 1x PBS, and then blocked in 10% normal goal serum (NGS) containing 0.3% Triton X-100 in 1x PBS for 1 h. Sections were incubated in rabbit anti-Dynorphin A 1–8 (Dyn-A, 1:500 (Vincent et al., 1982; Weber et al., 1982a; Weber et al., 1982b; Hollt, 1986; Gomes et al., 2020),) and guinea pig anti-NeuN (1:500, Synaptic Systems) in carrier solution (5% NGS in 0.1% Triton X-100 in 1x PBS) overnight at room temperature. After rinsing in 1x PBS, sections were incubated for 2 h in Alexa Flour 488-labeled goat anti-rabbit IgG and Alexa Flour 647-labeled goat anti-guinea pig IgG (both diluted 1:200). Finally, sections were rinsed in 1x PBS, dried, and cover-slipped with Prolong® mounting medium containing DAPI to permit visualization of nuclei. Background staining was assessed by omission of primary antibody in the immunolabeling procedure (negative control). LHb tissue sections of rats with previously established presence of Dyn-A/NeuN immunoreactive neurons were processed as positive control tissue. Images were captured using a Leica DMRXA Florescent Microscope.

Two 40x images of the LHb were taken at three AP location (−3.8, −3.9, and −4.1 relative to bregma). Using ImageJ sample pixel intensity, for each image, was averaged to include all pixels above of what was considered the “true” signal (35 pixel intensity). Background pixel averaging was performed to include all pixels below 35 pixel intensity. Density readings were created by normalizing all sample readings to background. The two normalized density reading from each AP location were averaged, and then each animal was averaged across AP location before group means were calculated.

2.7. qPCR

For all qPCR experiments we used similar procedures as published previously (Authement et al., 2018). Specifically, adolescent rats (PN21-28) were anesthetized using isofluorane and immediately decapitated. Brains were quickly dissected and placed in ice-cold ASCF

and sagittal slices were cut at 300 μm using a vibratome. All control ACSF treated slices were immediately grossly dissected to isolate 3–4 LHb tissues from both hemispheres and flash frozen in liquid nitrogen and stored at −80 °C until further processing. Total RNA was isolated using TRIzol (Life Technologies)/choloroform-based extraction. Samples were quantified using NanoDrop spectrophotometry at 260 and 280 nm optical densities. Reverse transcriptase amplification of cDNA from total RNA was conducted with High-Capacity RNA-to-cDNA kit (Applied Biosystems) and Bio-Rad CFX96 Real-Time System. TaqMan gene expression assays (Thermo Fisher Scientific) with probes for *Oprk1* (cat. Rn0144892_m1) and actin (Actb, cat. Rn00667869_m1) as a control for total RNA and the comparative C_T ($\Delta\Delta C_T$) were used to assess *Oprk1* expression in relation to *Actb* control, as described in (Authement et al., 2018). For each sample, the changes in target gene expression are given as $2^{-\Delta\Delta CT}$. All data were normalized to the non-MD group and presented as fold change.

2.8. Statistics

Values are presented as means ± SEM. The threshold for significance was set at *$p < 0.05$ for all analyses. All statistical analyses of data (2-tailed tests) were performed using Graphpad, Prism 8.4.1. For all electrophysiological data, n represents the number of recorded cells/rats. For detecting the difference in distribution of silent, tonic or bursting LHb neurons in non-MD and MD rats, we used Chi-square tests. For neuronal excitability data (number of APs generated across current step) with drug applications we used 2-way repeated measures (RM) ANOVA (RM in current step, and U50,488) of Ih- and Ih+ neurons separately. To assess baseline differences between Ih- and Ih+ neurons from non-MD rats or in comparison with those from MD rats (all in intact synaptic transmission), we used 2-way ANOVA. To assess whether all membrane and AP properties data (RMP, Rin, AP threshold, mAHP, fAHP, AP amplitude, and AP half-width) were normally distributed, we used the Shapiro-Wilk test ($\alpha = 0.05$) within each membrane/AP property across all data groupings (Ih and treatment). The effect of U50,488 on any AP/membrane properties were compared using Student's paired-t-test, or nonparametric Wilcoxon paired test where appropriate. Baseline differences between Ih- and Ih+ groups were compared using unpaired Student's t-test, or Mann-Whitney test (non-parametric data). All AP/membrane property group means ± SEM and result of statistical test results are summarized in table format (Supplemental Tables 1-3, 5-9). Supplemental Table 4 represents the summary of statistical analysis of the data in Supplemental Fig. 2.

Mini Analysis software was used to detect and measure mIPSCs and mEPSCs using preset detection parameters of mIPSCs and mEPSCs with an amplitude cutoff of 5 pA. Effects of U50,488 on the mean and cumulative probabilities of mEPSC and mIPSC amplitude and frequency data sets were analyzed using paired Student-t-tests and Kolmogorov-Smirnov tests ($\alpha = 0.05$), respectively.

The effects of MD on DynA (1–8) density were assessed using unpaired Student t-test. All qPCR data were analyzed first with Shapiro-Wilks test for normal distribution, followed by appropriate unpaired Student t-test, or nonparametric Mann-Whitney *U* test.

3. Results

3.1. KOR stimulation bidirectionally modulated LHb neuronal excitability

Compelling evidence implicates Dyn/KOR modulation of neuronal activity across a variety of reward/aversion processing brain regions (Crowley et al., 2016; Tejeda et al., 2017; Crowley and Kash, 2015; McLaughlin et al., 2003; Land et al., 2008) that also project to the LHb. However, up until now the role of KOR signaling in the LHb has not been investigated. Here, we first sought to establish whether activation of KORs can regulate LHb neuronal activity and synaptic function within the LHb and then investigate how ELS may modulate this signaling within the LHb.

For selective KOR stimulation throughout this study, we used a KOR-specific agonist (U50,488, 10 μM). First we tested the effects of U50,488 on LHb neuronal excitability by recording depolarization-induced AP generation in LHb neurons with intact synaptic transmission in slices from young-adolescent male rats (non-MD controls, PN21-28). We found that U50,488 had opposing effects on neuronal excitability in distinct LHb cell subpopulations (Fig. 1A–B) that were discriminated by the presence or absence of Ih currents (i.e., Ih+ versus Ih- LHb neurons). Fig. 1C depicts the average traces of Ih current recordings in response to a 50 mV hyperpolarizing voltage step from LHb neurons of all control (non-MD) rats recorded throughout this study (Ih-: n = 19/14; Ih+: n = 15/12) and a scatter plot of recorded Ih values across Ih- and Ih+ designations. U50,488 significantly decreased neuronal excitability in response to depolarization in Ih- LHb neurons as evident in the decreased average number of APs generated at each depolarizing current step compared to baseline levels (n = 13/10; 2-way RM ANOVA, effect of U50,488: $F(1,12) = 8.5$, $p < 0.05$; effect of current step: $F(9,108) = 10.4$, $p < 0.0001$; U50,488xcurrent interaction: $F(9,108) = 3.6$, $p < 0.001$) (Fig. 1A). Conversely, U50,488 significantly increased LHb neuronal excitability in Ih+ LHb neurons (n = 9/9, 2-way RM ANOVA, effect of U50,488: $F(1,8) = 9.2$, $p < 0.05$; effect of current step: $F(9,72) = 14.3$, $p < 0.0001$; U50,488xcurrent interaction: $F(9,72) = 4.8$, $p < 0.0001$) (Fig. 1B). In general, Ih+ baseline excitability was significantly higher than Ih- baseline excitability (2-way ANOVA, effect of Ih: $F(1,200) = 22.2$, $p < 0.0001$; effect of current: $F(9,200) = 4.0$, $p < 0.0001$; Ihxcurrent interaction $F(9,200) = 0.6$, $p > 0.05$, n.s.). Interestingly, we observed that the effects of U50,488 on LHb neuronal excitability persisted following a prolonged drug washout (data not shown). Although this may relate to a possible inability to completely wash the drug from the slice, it is also likely that acute KOR stimulation by U50,488 triggers a series of molecular adaptations in LHb neurons that induce and/or maintain a persistent change in neuronal excitability.

In addition to measuring the number of APs in response to depolarization following KOR stimulation, we also assessed the effects of U50,488 on several intrinsic passive and active membrane properties across both Ih- and Ih+ LHb neurons derived from the recordings reported in Fig. 1A–B (Fig. 1D–G and Supplemental Table 1). We found that at baseline levels, Ih- neurons had significantly higher input resistance (Rin) than Ih+ neurons (unpaired Student's t-test, $t(19) = 4.5$, $p < 0.001$, Fig. 1D) and U50,488 significantly altered Rin of Ih+ neurons only (paired *t*-test, $t(8) = 2.6$, $p < 0.05$, Fig. 1D). At baseline, AP thresholds of Ih- neurons was significantly lower (more depolarized) compared to Ih+ neurons (unpaired Student's t-test, $t(20) = 3.3$, $p < 0.01$, Fig. 1E). Irrespective of opposing effects on the excitability of Ih- and Ih+ neurons, stimulation of KOR by U50,488 lowered AP thresholds of both Ih- neurons (paired Student's t-test, $t(12) = 3.8$, $p < 0.01$, Fig. 1E) and Ih+ neurons (paired *t*-test, $t(8) = 3.5$, $p < 0.01$, Fig. 1E). U50,488 also significantly increased fAHPs in only Ih+ LHb neurons (paired Student's t-test, $t(8) = 2.7$, $p < 0.05$, Fig. 1F). At baseline, Ih- neurons had significantly larger mAHPs compared to Ih+ neurons (unpaired *t*-test, $t(20) = 2.8$, $p < 0.05$, Fig. 1G). U50,488 application significantly reduced mAHPs in both Ih- LHb neurons (paired Student's t-test, $t(12) = 3.9$, $p < 0.01$) and Ih+ LHb neurons (paired Student's t-test, $t(8) = 2.8$, $p < 0.05$, Fig. 1G).

To confirm that U50,488 acted through KORs to change LHb neuronal excitability, we then repeated these experiments in the presence of a novel KOR-specific antagonist provided by BlackThorn Inc., BTRX-084266 (here-on referred to as BTRX), and a validated KOR-specific antagonist, aticaprant. BTRX blocked the effects of U50,488 on both Ih- neurons (n = 3/3, 2-way RM ANOVA, effect of U50,488: $F(1,2) = 0.7$, $p > 0.05$, n.s.; effect of current: $F(9,18) = 2.0$, $p > 0.05$, n.s.; U50,488xcurrent interaction: $F(9,18) = 1.0$, $p > 0.05$ n.s., Fig. 2A) and Ih+ neurons (n = 4/4, 2-way RM ANOVA, effect of U50,488: $F(1,3) = 0.7$, $p > 0.05$, n.s.; effect of current: $F(9,27) = 1.4$, $p > 0.05$, n.s.; U50,488xcurrent interaction: $F(9,27) = 1.9$, $p > 0.05$, n.s. Fig. 2B).

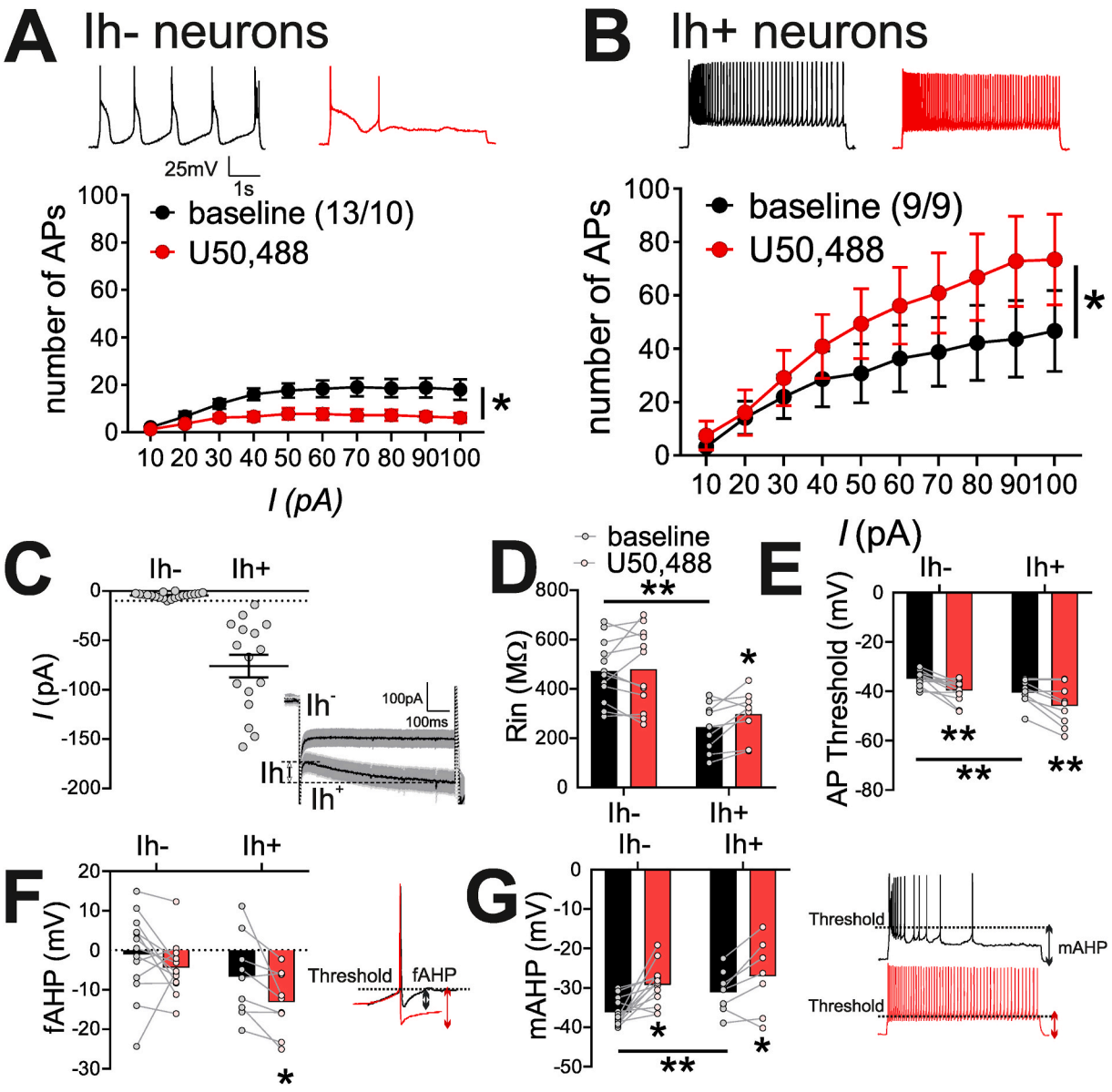

Fig. 1. KOR agonist, U50,488, bidirectionally altered LHb neuronal excitability in distinct subpopulations of LHb neurons identified by Ih currents. A-B, inset: Example traces of AP generation in response to +50 pA current injection at baseline (black) and post-U50,488 (red). A. U50,488 significantly decreased the number of AP generated across depolarizing current steps of Ih- neurons B. U50,488 significantly increased the number of AP generated across depolarizing current steps in Ih+ neurons C. Scatter plot of Ih values across Ih- (n = 20/15) and Ih+ (n = 16/13) groupings; Mean ± SEM displayed as bar/whisker; traces: Ih current traces (mean [line] ± SEM [shaded region]) in response to a hyperpolarizing voltage step from −50mV to −100mV in Ih- (≤-10 pA, n = 20/15) and Ih+ (>−10 pA, n = 16/13) groups. D. At baseline, Ih- neurons had larger input resistance (Rin) compared to Ih+ neurons and U50,488 treatment significantly increased Rin only in Ih+ neurons. E. At baseline, Ih- neurons had significantly lower (less negative) AP thresholds compared to Ih+ neurons. U50,488 significantly increased AP thresholds of both Ih- neurons and Ih+ neurons F. U50,488 induced a significant increase in fAHPs of Ih+ neurons, inset: sample traces for fAHPs before (black) and after the addition of U50,488 recorded from an Ih+ neuron in a non-MD control rat G. At baseline, Ih- neurons had significantly larger mAHP compared to Ih+ neurons. U50,488 significantly decreased mAHPs of Ih- neurons and Ih+ neurons. inset: sample traces for mAHPs before (black) and after the addition of U50,488 recorded from an Ih+ neuron in a non-MD control rat. *p < 0.05, **p < 0.01. In this and subsequent figures n represents the number of recorded cells/rats. (For interpretation of the references to colour in this figure legend, the reader is referred to the Web version of this article.)

Similarly, the effects of U50,488 were also blocked by aticaprant in both Ih- neurons (n = 5/4, 2-way RM ANOVA, effect of U50,488: $F(1,4) = 0.3$, $p > 0.05$, n.s.; effect of current: $F(9,36) = 1.4$, $p > 0.05$, n.s.; U50,488xcurrent interaction: $F(936) = 1.4$, $p > 0.05$, n.s.; Fig. 2C) and Ih+ neurons (n = 5/5, 2-way RM ANOVA; effect of U50,488: $F(1,4) = 2.0$ $p > 0.05$ n.s.; effect of current $F(9,36) = 9.4$, $p < 0.0001$; U50,488xcurrent interaction: $F(9,36) = 1.9$ $p > 0.05$ n.s.; Fig. 2D). Effects of both KOR antagonists on membrane and AP properties are summarized in Supplemental Tables 2–3, where both antagonists significantly blocked the effects of U50,488 on Rin and mAHP. In depolarization-induced AP recordings in the presence of KOR antagonists, we noticed that the higher basal levels of neuronal excitability of Ih+ neurons was absent. This prompted us to evaluate the effects of BTRX and aticaprant on spontaneous activity and firing patterns of LHb neurons as well as on basal levels of neuronal excitability in comparison to those recordings from non-MD controls with intact synaptic transmission. Due to the nature of cell-attached recordings where Ih currents cannot be measured and given that we could not measure Ih currents in all of our whole cell recordings, the distribution of spontaneous LHb neuronal activity and firing patterns are presented irrespective of Ih

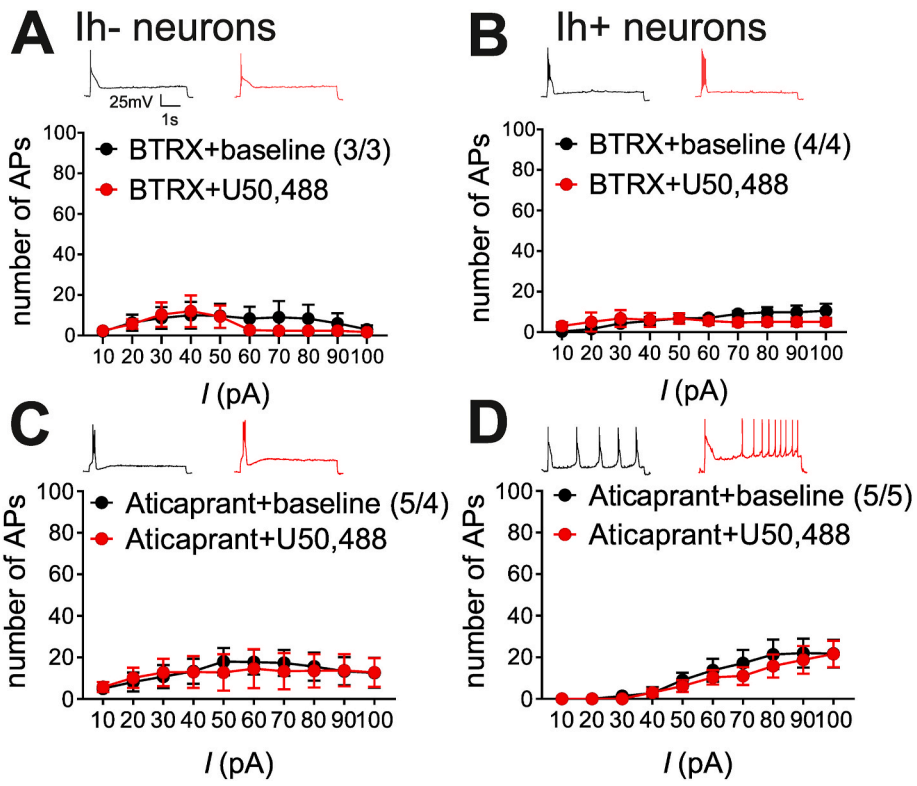

Fig. 2. KOR-specific antagonists, BTRX-084266 and aticaprant, blocked effects of U50,488 on LHb neuron excitability. Insets: Example traces of AP generation in response to +50 pA current injection at baseline + KOR antagonist (black) and post- KOR antagonist + U50,488 (red). A-B. Pretreatment with a KOR-specific antagonist, BTRX-084266 (BTRX), blocked U50,488-induced changes in the excitability in Ih- and Ih+ neurons C-D. Pretreatment with KOR-specific antagonist, aticaprant, blocked U50,488-induced changes in the excitability in Ih- and Ih+ neurons. (For interpretation of the references to colour in this figure legend, the reader is referred to the Web version of this article.)

categorization. We found that both antagonists significantly increased the proportion of bursting neurons compared to intact non-MD controls in whole cell-configuration and aticaprant also significantly increased the proportion of tonic firing neurons compared to non-MD controls in cell-attached configuration (controls in this figure are derived from recordings in Fig. 6, Supplemental Fig. 1). Furthermore, Ih+ baseline excitability was significantly lower in both BTRX and aticaprant compared to those from non-MD controls (controls in this figure are derived from recordings in Fig. 1, Supplemental Fig. 2, Supplemental Table 4). Additionally, Ih- baseline excitability was significantly lower in only BTRX (Supplemental Fig. 2, Supplemental Table 4). To our knowledge this is the first demonstration of functional KOR signaling in the LHb neuron excitability.

3.2. *The effects of KOR stimulation on LHb neuronal excitability required intact fast synaptic transmission*

Changes in both LHb neuronal intrinsic properties as well as synaptic transmission may drive the differential KOR modulation of LHb neuronal excitability in Ih- and Ih+ neurons. Therefore, we next tested whether KOR stimulation by U50,488 induces any change in intrinsic neuronal excitability in the absence of fast synaptic transmission (SynBl) by blocking AMPARs, NMDARs and $GABA_A$Rs in slices from non-MD control rats. Under these conditions we observed that stimulation of KOR by U50,488 did not significantly affect neuronal excitability in response to depolarization in Ih- ($n = 9/7$; 2-way RM ANOVA, effect of U50,488: $F(1,8) = 1.7$, $p > 0.05$, n.s.; effect of current: $F(9,72) = 2.1$, $p < 0.05$; U50,488xcurrent interaction: $F(9,72) = 1.1$, $p > 0.05$, n.s.) nor in Ih+ LHb neurons ($n = 7/7$; 2-way RM ANOVA, effect of U50,488: $F(1,6) = 0.5$, $p > 0.05$, n.s.; effect of current $F(9,54) = 2.1$, $p < 0.05$; U50,488xcurrent interaction: $F(9,54) = 0.2$, $p > 0.05$, n.s.; Fig. 3A–B). Interestingly, under synaptic blockade conditions, some of our findings for KOR-mediated changes in intrinsic membrane properties persisted or were otherwise uncovered. For example, while we found that Ih- LHb neurons still exhibited a higher Rin compared to Ih+ LHb neurons, U50,488 now significantly increased the Rin of Ih- neurons. U50,488 also significantly lowered AP threshold, increased fAHPs and significantly decreased mAHPs in both Ih- and Ih+ neurons (Supplemental Table 5).

In order to determine the necessity of specific glutamatergic and GABAergic receptors for U50,488-induced alteration of excitability, experiments were repeated with each synaptic receptor blocked individually in slices from non-MD controls rats. Application of AMPAR antagonist (DNQX) significantly blocked effects of U50,488 on Ih- neurons ($n = 4/4$, 2-way RM ANOVA, effect of U50,488: $F(1,3) = 0.7$, $p > 0.05$ n.s.; effect of current: $F(9,27) = 1.2$, $p > 0.05$, n.s.; U50,488xcurrent interaction: $F(9,27) = 0.9$, $p > 0.05$ n.s.; Fig. 3C). In comparison, U50,488 effect on Ih+ LHb neurons remained intact in the presence of DNQX ($n = 7/5$; 2-way RM ANOVA; effect of U50,488: $F(1,6) = 6.3$, $p < 0.05$; effect of current: $F(9,54) = 9.9$, $p < 0.0001$; U50,488xcurrent interaction: $F(9,54) = 3.5$, $p < 0.01$, Fig. 3D). Blockade of NMDARs using APV significantly blocked Ih- LHb response to U50,488 (n5/4; 2-way RM ANOVA, effect of U50,488: $F(1,4) = 0.4$, $p > 0.05$ n.s.; effect of current: $F(9,36) = 7.0$, $p < 0.0001$; U50,488xcurrent interaction: $F(9,36) = 0.6$, $p > 0.05$, n.s.; Fig. 3E). Similarly, APV application also blocked Ih+ LHb response to U50,488 ($n = 8/8$; 2-way RM ANOVA; effect of U50,488: $F(1,7) = 0.3$, $p > 0.05$, n.s.; effect of current $(9,63) = 4.9$, $p < 0.0001$; U50,488xcurrent interaction: $F(9,63) = 0.5$, $p > 0.05$, n.s.; Fig. 3F).

Individual blockade of $GABA_A$Rs (PTX application) prevented the effects of U50,488 on Ih- ($n = 5/4$, 2-way RM ANOVA; effect of U50,488: $F(1,4) = 1.1$ $p > 0.05$ n.s.; effect of current $F(9,36) = 0.9$, $p > 0.05$, n.s.; U50,488xcurrent interaction: $F(9,36) = 0.5$, $p > 0.05$ n.s.; Fig. 3G) and Ih+ LHb neurons ($n = 5/4$; 2-way RM ANOVA; effect of U50,488: $F(1,4) = 0.3$, $p > 0.05$, n.s.; effect of current: $F(9,36) = 11.8$, $p < 0.0001$; U50,488xcurrent interaction: $F(9,36) = 0.2$, $p > 0.05$ n.s.; Fig. 3H). Effects of U50,488 across complete synaptic blockade (SynBl) and each synaptic blocker (APV, DNQX, and PTX) on membrane and AP properties are summarized in Supplemental Tables 5–8, respectively. Some of these changes induced by KOR activation in intact conditions also

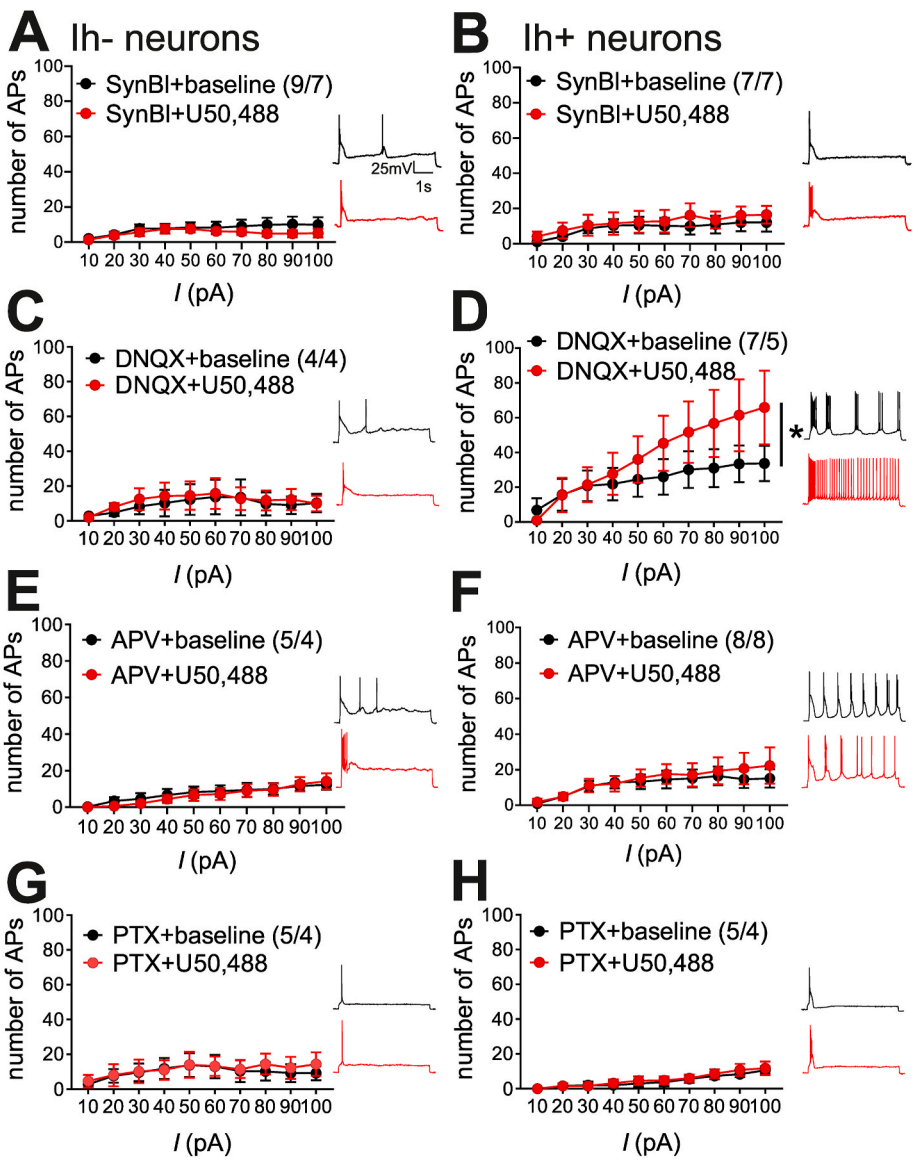

Fig. 3. Effects of U50,488 on LHb neuronal excitability required intact synaptic transmission. Insets: Example traces of AP generation in response to +50 pA current injection at baseline + synaptic receptor blocker/s (black) and post-synaptic receptor blocker/s + U50,488 (red). A-B. Complete fast-synaptic blockade of $GABA_A$Rs (PTX), NMDARs (APV), and AMPARs (DNQX) (collectively referred to as SynBl) blocked the effects of U50,488 on AP generated across depolarizing current steps in Ih- and Ih+ neurons. C. DNQX prevented the effects of U50,488 in Ih- neurons D. U50,488 effect on excitability of Ih+ neurons remained intact with DNQX application. E-F. APV application blocked the effects of U50,488 in Ih- and Ih+ neurons. G-H. PTX application blocked the effects of U50,488 in Ih- and Ih+ neurons. *$p < 0.05$. (For interpretation of the references to colour in this figure legend, the reader is referred to the Web version of this article.)

persisted in the presence of synaptic receptor blockers, although the main finding was related to the induction of similar changes by U50,488 in AP threshold (more negative) and mAHPs (lower levels) of Ih+ neurons that were still responsive to the stimulatory of KOR activation.

Given that fast synaptic transmission mediated by AMPARs, NMDARs or $GABA_A$Rs could contribute to spontaneous LHb activity with different firing patterns and the maintenance of baseline excitability of Ih- and Ih+ LHb neurons, we also evaluated the effects of complete synaptic blockade and each receptor blocker individually on LHb spontaneous activity and firing patterns (Supplemental Fig. 1) as well as on basal levels of neuronal excitability of Ih- and Ih+ neurons (Supplemental Fig. 2). Briefly, we found that while complete synaptic blockade (SynBl) did not alter spontaneous activity, APV and PTX (but not DNQX) significantly increased the overall activity of LHb neurons with a larger proportion of burst-firing neurons in both cell-attached and whole cell configuration compared to intact conditions (Supplemental Fig. 1 with intact controls derived from Fig. 6). At further inspection, APV and PTX (but not DNQX) application significantly reduced the excitability of both Ih- and Ih+ neurons compared to intact conditions (Supplemental Fig. 2, Supplemental Table 4). In contrast, DNQX did not significantly affect baseline excitability of Ih+ neurons which was comparable to intact control conditions (Supplemental Fig. 2, Supplemental Table 4). Supplemental Tables 5–8 provide summaries of basal membrane and AP properties across complete SynBl, APV, DNQX, and PTX, respectively. Consistent with persistence of higher basal excitability of Ih+ neurons in DNQX conditions, the difference in basal levels of Rin between Ih- and Ih+ neurons was also present with Ih+ neurons having a significantly lower Rin levels.

3.3. *KOR stimulation altered both glutamatergic and GABAergic synaptic transmission within the LHb*

To directly test the effects of KOR signaling on synaptic transmission, we next tested the effects of U50,488 on AMPAR-mediated mEPSC (Fig. 4) and $GABA_A$R-mediated mIPSC (Fig. 5). It should be mentioned that recording of Ih is not feasible under mEPSC and mIPSC recordings given the necessary pharmacological manipulations and internal solutions required for these types of recordings also directly block or alter Ih currents. Therefore Ih- and Ih+ LHb neurons could not be distinguished in these recordings. We observed that U50,488 had a consistent yet trending decrease in the mean amplitude of mEPSCs ($n = 10/10$, paired Student's t-test, $t(9) = 2.1$ $p = 0.07$) as well as a significant change in cumulative probability of mEPSC amplitude (Kolmogorov-Smirnov [KS] test, $p < 0.0001$; Fig. 4A). Moreover, we found a significant reduction in

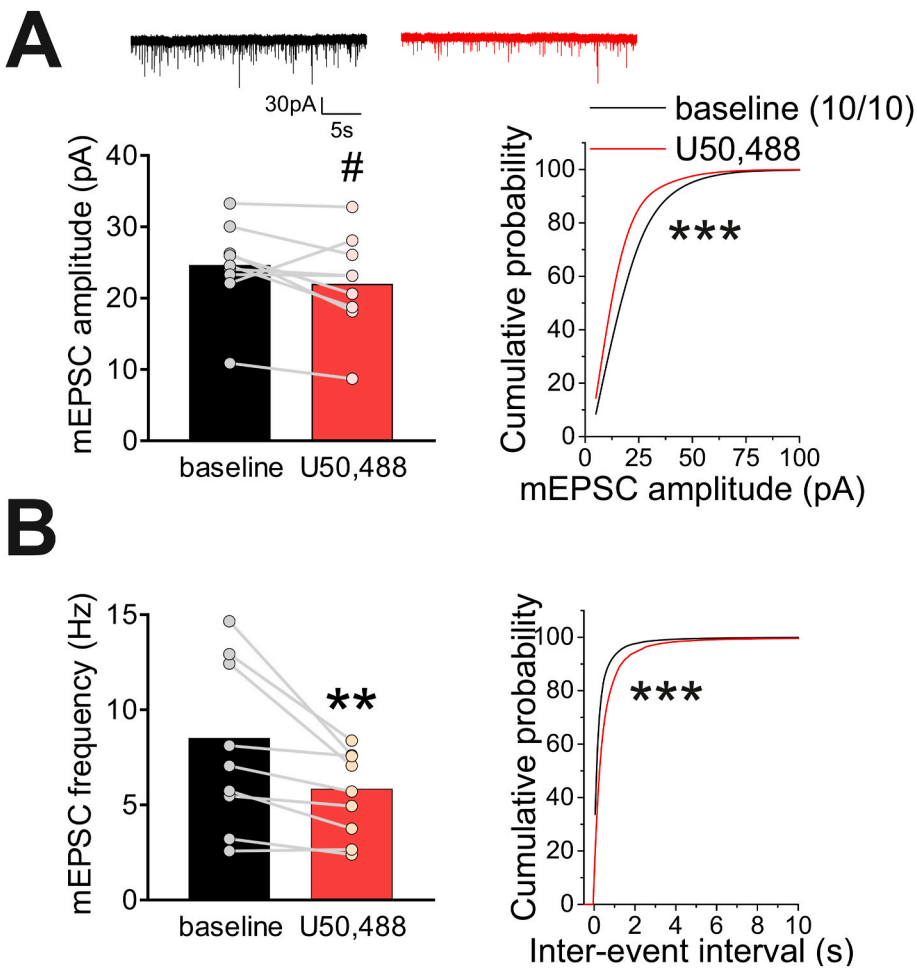

Fig. 4. U50,488 suppressed glutamatergic transmission onto LHb neurons. A. Top: representative AMPAR-mediated mEPSC traces recorded from LHb neurons before (baseline, black) and after U50,488 (10 μM, red) application. U50,488 had a trending decrease in the mean amplitude of mEPSCs but significantly decreased cumulative probability of mEPSC amplitude. B. U50,488 treatment decreased the average mEPSC frequency and cumulative probability of inter-event intervals of mEPSCs. #p = 0.066, **p < 0.01, ***p < 0.0001. (For interpretation of the references to colour in this figure legend, the reader is referred to the Web version of this article.)

the mean frequency of mEPSCs (n = 10/10, paired Student's t-test, t(9) = 3.4, p < 0.05) as well as a significant decrease in the cumulative probability of mEPSC inter-event interval (IEI) following U50,488 treatment (KS test, p < 0.0001; Fig. 4B). These findings indicate that KOR stimulation uniformly suppresses glutamatergic transmission within the LHb, significantly diminishing both presynaptic glutamate release and also decreasing postsynaptic AMPAR function (the number of AMPARs and/or the conductance of AMPARs) in LHb neurons.

In contrast to the consistent effects of KOR stimulation on glutamatergic transmission, the effects of U50,488 on GABAergic transmission was varied. Overall, U50,488 significantly reduced the mean amplitude of mIPSCs (n = 14/8; paired Student's t-test; t(13) = 3.5, p < 0.01) and cumulative probability plots of mIPSC amplitude (KS test, p < 0.0001; Fig. 5A). In contrast, in 10 out of the 14 neurons U50,488 significantly decreased mean mIPSC frequency (n = 10/8, paired Student's *t*-test, t(9) = 3.9, p < 0.01) and cumulative probability mIPSC frequency (KS test, p < 0.0001; Fig. 5B). On the other hand, in 4 out of the 14 neurons U50,488 significantly increased both mean (n = 4/4, one-tail paired *t*-test, t(3) = 2.4, p < 0.05) and cumulative probability of mIPSC frequency (KS test, p < 0.0001; Fig. 5C).

3.4. MD altered sensitivity of LHb neurons to KOR signaling

Previously we observed that MD blunts responses of LHb neurons to CRF signaling (Authement et al., 2018). Given that dysregulation of Dyn/KOR modulation of DA circuits following stress including ELS is shown to mediate part of central CRF stress response or act in concert with CRF to promote drug-induced synaptic plasticity, drug seeking behaviors and stress-induced reinstatement (Tejeda and Bonci, 2019; Bruchas et al., 2010; Karkhanis et al., 2016; Land et al., 2008; Mantsch et al., 2016; Pautassi et al., 2012), we hypothesized that Dyn/KOR signaling within the LHb may also be dysregulated following MD stress. First, we recorded the spontaneous activity and firing patterns of LHb neurons in non-MD and MD rats in both cell-attached and whole cell recordings of APs with intact synaptic transmission to confirm our previous findings that MD significantly increases spontaneous LHb neuronal activity (Authement et al., 2018). We found that MD increased LHb spontaneous activity with more prevalence of active neurons in tonic and bursting modes of firing compared to non-MD controls in young-adolescent male rats (PN21-28) (cell-attached voltage clamp: non-MD, n = 127/54; MD, n = 93/48; whole cell Current Clamp: non-MD, n = 119/25; MD: n = 105/46; Chi squared test, ***p < 0.0001, Fig. 6). As mentioned earlier, we acknowledge that we could not measure Ih currents in all of our whole cell recordings for spontaneous LHb neuronal activity. However, upon successful measurements of Ih in some of LHb neurons from non-MD and MD rats, we found an equal distribution of these currents across different modes of neuronal activity and firing patterns (data not shown).

We then tested the effects of KOR stimulation by U50,488 on LHb neuronal excitability with intact synaptic transmission in MD rats (Fig. 7A–B) similar to experiments conducted in non-MD intact controls in Fig. 1. Importantly, there was no significant difference in regard to the amplitude of Ih+ currents between Ih+ LHb neurons of non-MD and MD rats (non-MD Ih+: n = 15; MD Ih+: n = 30; Mann-Whitney test, p > 0.05, n.s.; Fig. 7C), nor a significant difference between amplitude of Ih- currents (non-MD Ih-: n = 18; MD Ih-: n = 18, Mann-Whitney test, p > 0.05, n.s.; Fig. 7C) suggesting a similar distribution of Ih across LHb neurons. Strikingly, we found that MD completely abolished the effects

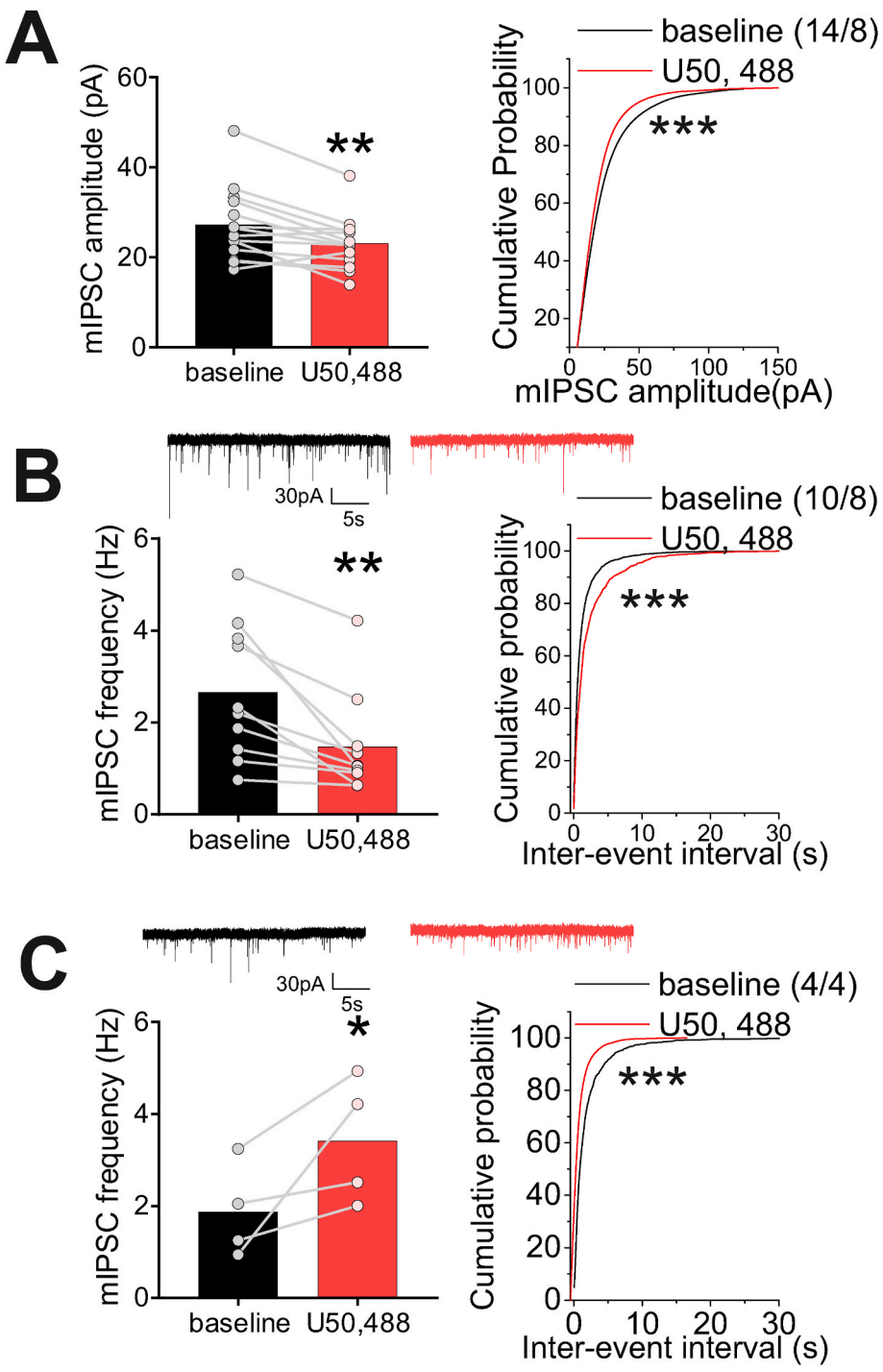

Fig. 5. U50,488 altered GABAergic synaptic transmission onto LHb neurons. A. U50,488 decreased the mean amplitude of mIPSCs and decreased the cumulative probability of mIPSC amplitude. B. Representative mIPSC traces at baseline (black) and following U50,488 treatment (red). Out of 14 recorded cells from A., U50,488 treatment decreased the average of mIPSC frequency as well as the cumulative probability of inter-event intervals of mIPSCs in 10 recorded cells. C. Representative mIPSC traces at baseline (black) and following U50,488 treatment (red). Out of 14 recorded cell in A., U50,488 treatment increased the average frequency and the cumulative probability of inter-event intervals of mIPSCs in 4 recorded cells (n = 4/4). *p < 0.05, **p < 0.01, ***p < 0.0001. (For interpretation of the references to colour in this figure legend, the reader is referred to the Web version of this article.)

of U50,488 on neuronal excitability in both Ih- (n = 8/7, 2-way RM ANOVA, effect of U50,488: $F(1,7) = 0.04$, $p > 0.05$, n.s.; effect of current: $F(9,63) = 10.7$ $p < 0.0001$; U50,488xcurrent interaction: $F(9,60) = 0.3$, $p > 0.05$, n.s., Fig. 7A) and Ih+ neurons (n12/11; 2-way RM ANOVA, effect of U50,488: $F(1,11) = 0.8$, $p > 0.05$ n.s.; effect of current: $F(9,99) = 3.7$ $p < 0.001$; U50,488xcurrent interaction: $F(9,99) = 1.5$, $p > 0.05$, n.s.; Fig. 7B). Interestingly, the baseline excitability of MD Ih+ neurons were significantly lower than those of non-MD controls in intact synaptic transmission mimicking the conditions where NMDARs and $GABA_A$Rs were blocked (Supplemental Fig. 2, Supplemental Table 4). Although the baseline difference of Rin between Ih- and Ih+ neurons that we observed with control non-MD rats was still present in MD rats (Mann-Whitney test, $p < 0.01$ Fig. 7D), U50,488 treatment did not affect Rin in either population (Ih-: Wilcoxon test, $p > 0.05$ n.s.; Ih+: Wilcoxon test, $p > 0.05$; Fig. 7D). While there was no observed baseline difference between MD AP threshold of Ih- and Ih+ neurons (Mann-Whitney test, $p > 0.05$, n.s.), U50,488 significantly increased AP thresholds in both MD Ih-neurons (Wilcoxon paired test, $p < 0.01$) and MD Ih+ neurons (paired Student's t-test, $t(11) = 2.4$ $p < 0.05$) (Fig. 7E). Unlike the intact conditions in non-MD controls, there was no significant effect of U50,488 nor baseline difference between fAHPs of Ih- (paired *t*-test, $t(7) = 1.8$, $p > 0.05$ n.s.) and Ih+ (paired *t*-test, $t(11) = 1.7$, $p > 0.05$, n.s.) neurons in MD rats (Fig. 7F). U50,488 significantly reduced mAHPs of both Ih- (paired Student's t-test, $t(7) = 4.3$, $p < 0.01$) and Ih+ LHb neurons

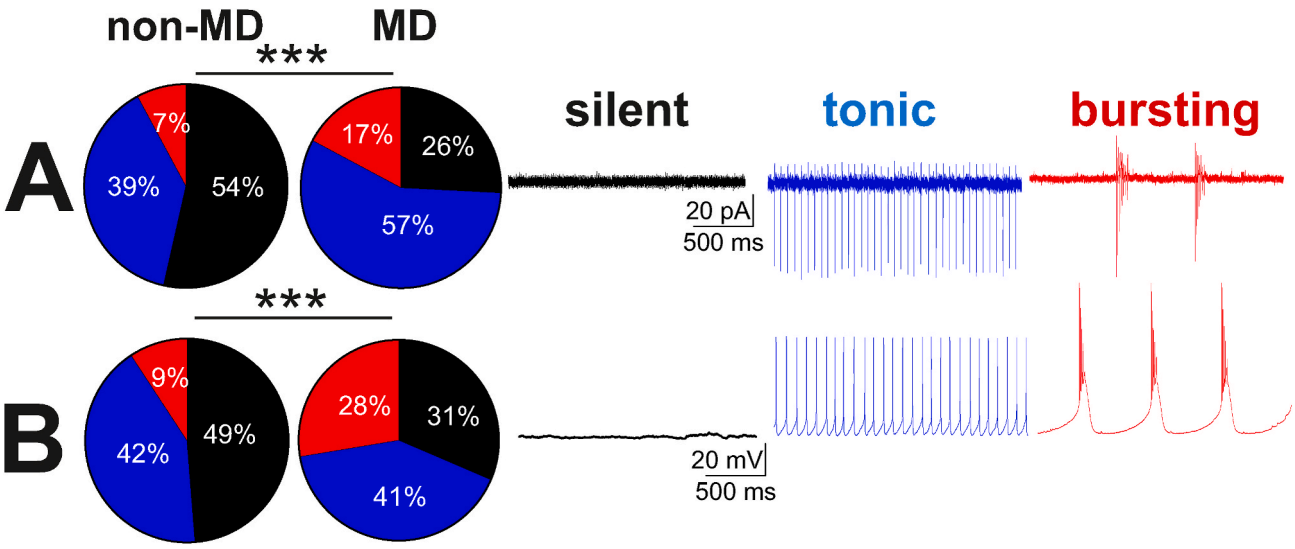

Fig. 6. MD increased spontaneous activity of LHb neurons. A-B, Pie charts with representative traces of A. voltage-Clamp (VC, V = 0) cell-attached recordings and B. current clamp (CC, I = 0) whole-cell recordings of spontaneous neuronal activity across non-MD and MD rats. Comparison of the percent distributions of silent (black), tonic (blue), or bursting (red) LHb neurons showed a significant increase in tonic and bursting LHb neuronal activity following MD. ***p < 0.0001. (For interpretation of the references to colour in this figure legend, the reader is referred to the Web version of this article.)

(paired Student's t-test, $t(11) = 4.1$, $p < 0.01$) in MD rats similar to non-MD controls in Fig. 1 (Fig. 7G). Supplemental Table 9 provides a summary of basal intrinsic membrane and AP properties of Ih- and Ih+ neurons following MD in intact synaptic transmission. Considering that the effects of KORs on LHb neuronal excitability of non-MD control rats was absent when fast synaptic transmission, NMDARs or $GABA_A$Rs were blocked (Fig. 3), the absence of these effects in MD rats suggests that the presynaptic effects of KOR stimulation on LHb neuronal excitability may be inhibited or occluded following MD. To directly address this, we next examined possible MD-induced alterations in basal Dyn/KOR signaling.

3.5. MD dysregulated DYN/KOR signaling within the LHb

The observed lack of LHb neuronal responses to KOR stimulation following MD may be due to changes in the expression of Dyn/KOR system or defective KOR downstream signaling. Therefore, we first examined whether MD alters the expression of Dyn-A (an endogenous opioid peptide that activates KORs with high potency) within the LHb. We performed double immunofluorescence with antibodies against NeuN (neuron-specific marker) and DYN-A(1–8) (an antibody specific to vesicular Dyn-A peptides) on male young-adolescent rats (PN28). Representative images of immuno-labeled DYN-A(1–8) highlight that the expression of this peptide was mainly seen within fibers across LHb (Fig. 8A). We found that MD significantly and consistently increased Dyn-A(1–8) density not only in PN28 (non-MD: n = 10; MD: n = 9; unpaired Student's t-test, $t(17) = 4.6$, **$p < 0.001$), but also in Juveniles (PN16) as well as adult (PN60) MD rats compared to non-MD (age-matched) indicating a persistent elevation in Dyn expression across development (Supplemental Fig. 3).

Given MD-induced DYN signaling hypertrophy, it is possible that the lack of LHb neuronal responses to KOR stimulation of MD rats is driven by a downregulation of KORs in response to persistent activation of these receptors by hypertrophied Dyn transmission or alteration in signaling pathways down-stream of Dyn/KOR (Margolis and Karkhanis, 2019; Tejeda and Bonci, 2019; Ehrich et al., 2015; Crowley et al., 2016; Tejeda et al., 2017; Bruchas and Chavkin, 2010). In order to assess MD-induced alterations in the expression of KORs, we measured KOR mRNA abundance using qPCR. We found a significant decrease in *oprk1* (opioid peptide receptor kappa-1) mRNA expression in LHb tissues from MD rats compared to non-MD controls (non-MD n = 11, MD n = 9; unpaired student t-test, $t(18) = 3.4$, $p < 0.01$, Fig. 8B).

4. Discussion

Previously, we reported that the stress neuromodulator, CRF, acts through CRF receptor 1 (CRFR1)-protein kinase A (PKA) to increase LHb neuronal excitability uniformly across all LHb neurons (Authement et al., 2018). In contrast to this consistent excitatory response of LHb neurons to CRF, here we establish a role for another stress modulatory system, Dyn/KOR signaling, that exerted differential effects on the excitability of two functionally discrete LHb neuronal subpopulations suggesting a cell-specific modulation of neuronal activity within the LHb by this stress system. We found that LHb neurons discriminated based on the absence or presence of Ih currents responded with a decrease or an increase in excitability (Ih- and Ih+ neurons, respectively) to KOR stimulation primarily through presynaptic KOR modulation of glutamatergic and GABAergic inputs within the LHb. Although the majority of LHb neurons are believed to be glutamatergic, there is more appreciation for anatomically and/or functionally diverse neuronal populations within the LHb that receive distinct synaptic inputs and projections to segregated and non-overlapping targets including the VTA, substantia nigra compacta, rostromedial tegmental area (RMTg), or raphe nuclei (RN), thus comprising distinct neural circuits that control motivational behaviors (Hu et al., 2020; Cerniauskas et al., 2019; Wallace et al., 2017; Stamatakis et al., 2016; Lecca et al., 2020). Almost all LHb neurons projecting to the VTA or RN appear to express all four HCN subunits (Poller et al., 2011), however, a later study found that only a subset of glutamatergic medial LHb (mLHb) neurons with functional Ih are excited by DA-D4R activation of Ih currents and these neurons project to the RMTg but not to the VTA (Good et al., 2013). Interestingly, there is also an emerging and controversial notion of the existence of a small population of functional GABAergic interneurons within the LHb that locally suppress neuronal activity to increase motivation (Zhang et al., 2016, 2018; Webster et al., 2020). Although whether the Ih- and Ih+ neurons identified in this study are glutamatergic or GABAergic remains to be directly assessed, we propose a model for cell-specific KOR-dependent neuromodulation of LHb microcircuit (Fig. 9) where Ih- neurons serve as the GABAergic interneurons that provide local inhibition to Ih+ glutamatergic neurons. Therefore, in this model, aversive or stressful stimuli can engage these distinct LHb neuronal populations through selective KOR-mediated activation of Ih+ glutamatergic neurons and/KOR-mediated inhibition of Ih- GABAergic interneurons, ultimately increasing the activity in glutamatergic output

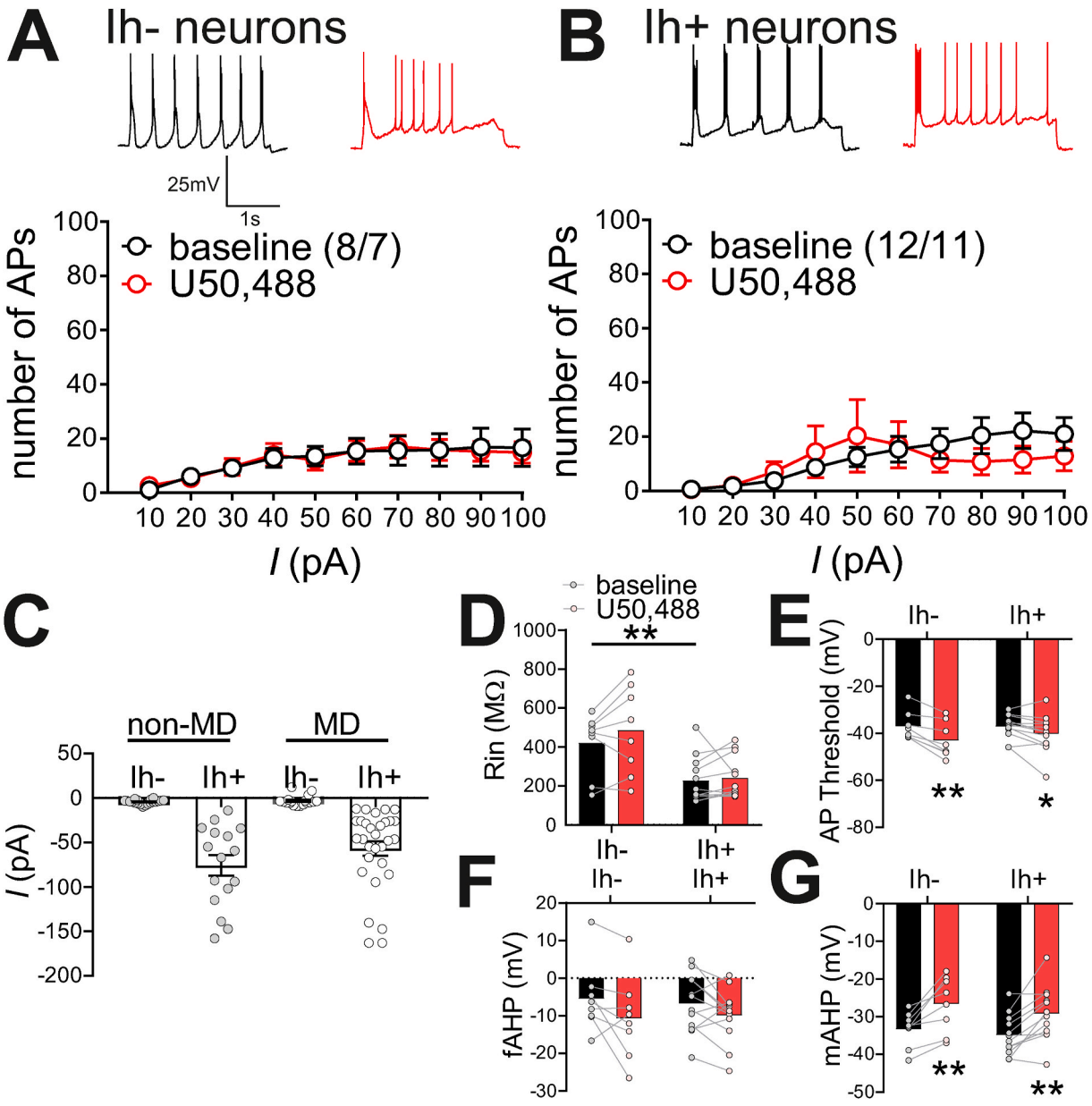

Fig. 7. Effects of U50,488 on LHb neuronal excitability were absent following MD. A-B. Example traces of AP generation in response to +50 pA current application at baseline (black) and 30min post- U50,488 (red). U50,488 did not significantly alter the number of AP generated across depolarizing current steps of A. Ih- neurons or B. Ih+ neurons in MD rats. C. Scatter plot of Ih currents recorded from LHb neurons across non-MD (grey) and MD (white) rats (non-MD, Ih-: n = 19/14; MD, Ih-: n = 8/7; non-MD, Ih+: n = 15/12; MD, Ih+: n = 12/10). There was no significant difference in the mean amplitude of Ih currents in Ih+ LHb neurons between non-MD and MD rats. D. At baseline, MD Ih- neurons had larger Rin compared to MD Ih+ neurons. E. U50,488 significantly lowered AP thresholds in both MD Ih- neurons and MD Ih+ neurons F. There was no effect of U50,488 on fAHPs in MD Ih- or MD Ih+ neurons. G. U50,488 significantly decreased mAHPs of both MD Ih- neurons and MD Ih+ neurons. *p < 0.05, **p < 0.01, ***p < 0.0001. (For interpretation of the references to colour in this figure legend, the reader is referred to the Web version of this article.)

pathways that suppresses motivational behaviors, and promotes avoidance.

The two subpopulations of LHb neurons (i.e., Ih- and Ih+ LHb neurons) differed in their basal levels of activity as well as their intrinsic membrane properties, and their responses to KOR stimulation. We found that with intact synaptic transmission KOR stimulation decreased the excitability of Ih- neurons while did the opposite in Ih+ neurons. The ability of KORs in modulating the neuronal excitability was abolished in the absence of synaptic transmission in both Ih- and Ih+ neurons suggesting that KOR-induced modulation of LHb neuronal excitability are mainly mediated through presynaptic KORs expressed on synaptic inputs. This conclusion was further substantiated by our findings from mEPSC and mIPSC recordings where we found that KOR stimulation predominantly decreased presynaptic glutamate release onto LHb neurons while it could either decrease (in majority of LHb neurons) or increase (in a small number of LHb neurons) GABA release onto LHb neurons. Given that the effects of KOR stimulation on postsynaptic $GABA_AR$-mediated synaptic function was consistently diminished across almost all LHb neurons similar to the effects observed with postsynaptic AMPAR-mediated synaptic function, the variable effects of KOR signaling on presynaptic GABA release may suggest a projection-specific rather than a cell type-specific modulation of GABAergic synaptic transmission by presynaptic KOR signaling. In contrast to presynaptic effects of KOR signaling in LHb neurons, CRF-induced increases in LHb

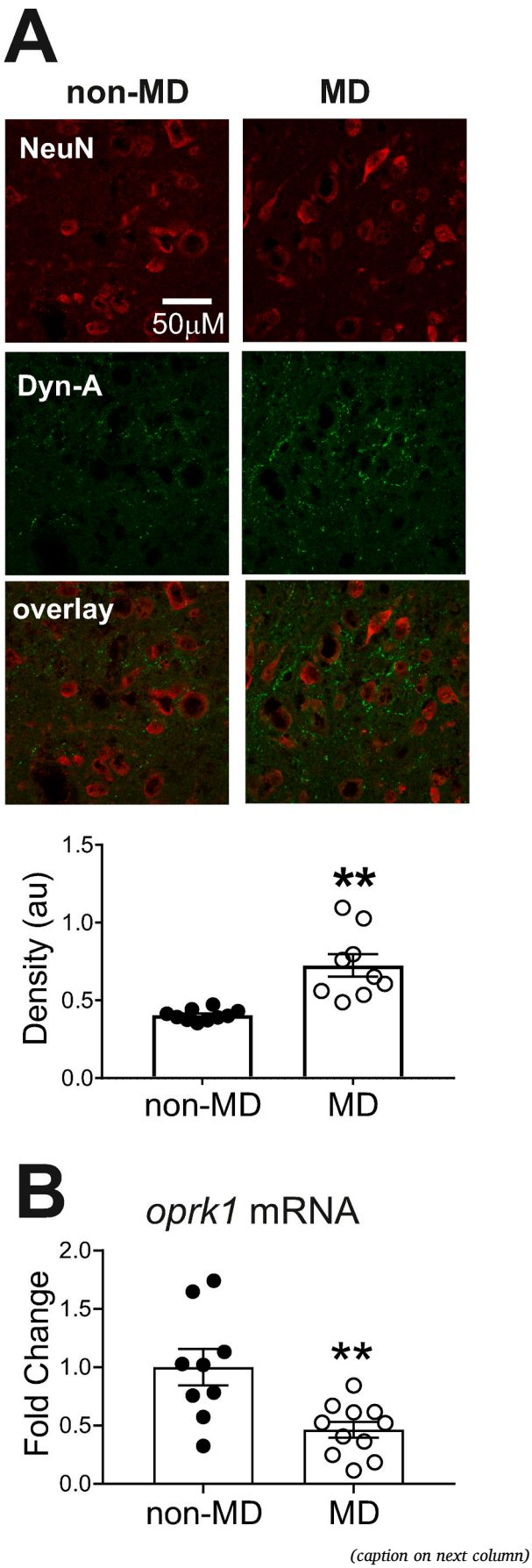

(caption on next column)

Fig. 8. MD altered Dyn-A peptide and KOR expression in the LHb. A. Example images of non-MD (left) and MD (right) immunolabeling for LHb neurons (NeuN, red, top), Dyn-A(1–8) peptide (green, middle) and merged overlay images (bottom panel). Scale bar = 50 μm. MD significantly increased average LHb Dyn-A density compared to non-MD controls B. LHb of MD rats had significantly lower abundance of opioid peptide receptor, kappa 1 (*oprk1*) mRNA expression compared to non-MD controls. **p < 0.01. (For interpretation of the references to colour in this figure legend, the reader is referred to the Web version of this article.)

excitability is present in the presence or absence of fast synaptic transmission and are primarily mediated through changes in intrinsic small- and large-conductance SK- and BK-type K+ channels, although CRF's excitatory effects on LHb excitability could also be supported by CRF-induced reduction of GABA release onto LHb neurons by endocannabinoid (eCB)-mediated retrograde signaling (Authement et al., 2018). In contrast, opioid receptors including KORs in general inhibit neurotransmitter release through Gi/Go G-protein-coupled signaling (Crowley and Kash, 2015) which may support a model of disinhibition of Ih+ neurons through suppression of GABAergic synapses onto LHb neurons. But it is still possible that the excitatory actions of KORs in Ih+ excitability are also mediated through promotion of eCB production which reduces GABA release from presynaptic terminals in the LHb. Interestingly, the complete blockade of fast synaptic transmission not only blocked KOR-induced modulation of LHb excitability but also dampened the levels of excitability of both Ih- and Ih+ neurons without any change in the overall spontaneous activity and firing patterns of LHb neurons. This suggested that AMPARs, NMDARs and $GABA_A$Rs may be required for the maintenance of LHb neuronal excitability and mediate KOR effects. To identify the individual contribution of each synaptic component in basal activity and KOR responses, we then pharmacologically blocked either AMPARs, NMDARs or $GABA_A$Rs and examined the overall spontaneous activity and firing patterns of LHb neurons (although irrespective of Ih categorization) and the neuronal excitability in response to depolarization of Ih- and Ih+ neurons (before and after the addition of the selective KOR agonist, U50, 488). In general, Ih+ neurons exhibited high frequency tonic level of neuronal excitability in response to depolarization while Ih- neurons were overall less active and usually exhibited a bursting response during depolarization. The baseline high frequency tonic AP generation in Ih+ neurons was dependent on activation of either NMDARs or $GABA_A$Rs but not AMPARs. Blockade of either NMDARs or $GABA_A$Rs also prevented the excitatory effects of KOR stimulation on Ih+ LHb excitability while blockade of AMPARs did not. On the other hand, Ih- neuronal excitability was diminished by the blockade of either AMPARs, NMDARs or $GABA_A$Rs and each of these synaptic manipulations was sufficient to block the inhibitory effects of KOR stimulation on Ih-neuronal excitability. While activation of post-synaptic excitatory receptors (both AMPARs and NMDARs in Ih- neurons, and only NMDARs in Ih+ neurons) could provide neuronal excitation in both neuronal subtypes, the effects of $GABA_A$R blockade to decrease excitability of Ih- and Ih+ neurons seemed puzzling given that a lesser $GABA_A$R-mediated inhibition should trigger neuronal excitation. However, further analysis of basal spontaneous activity and firing patterns in each of these synaptic manipulations revealed that with blockade of either NMDARs or $GABA_A$Rs (but not AMPARs), increased the number of spontaneously active LHb neurons in both tonic and bursting mode, specifically there was a transition in firing patterns of LHb neurons with a larger number of active LHb neurons that fired in bursting mode. In general, LHb patterns of spontaneous firing is highly sensitive to changes in membrane potential and the neurons are able to switch their firing patterns from tonic or silent to bursting or vice versa (Yang et al., 2018a; Wagner et al., 2017; Weiss and Veh, 2011). Also it is important to note that bursting LHb neurons have a more negative RMP than silent and tonic-firing neurons which we have also observed in our recordings. The promotion of bursting activity by the blockade of the inhibitory $GABA_A$Rs could promote membrane depolarization necessary

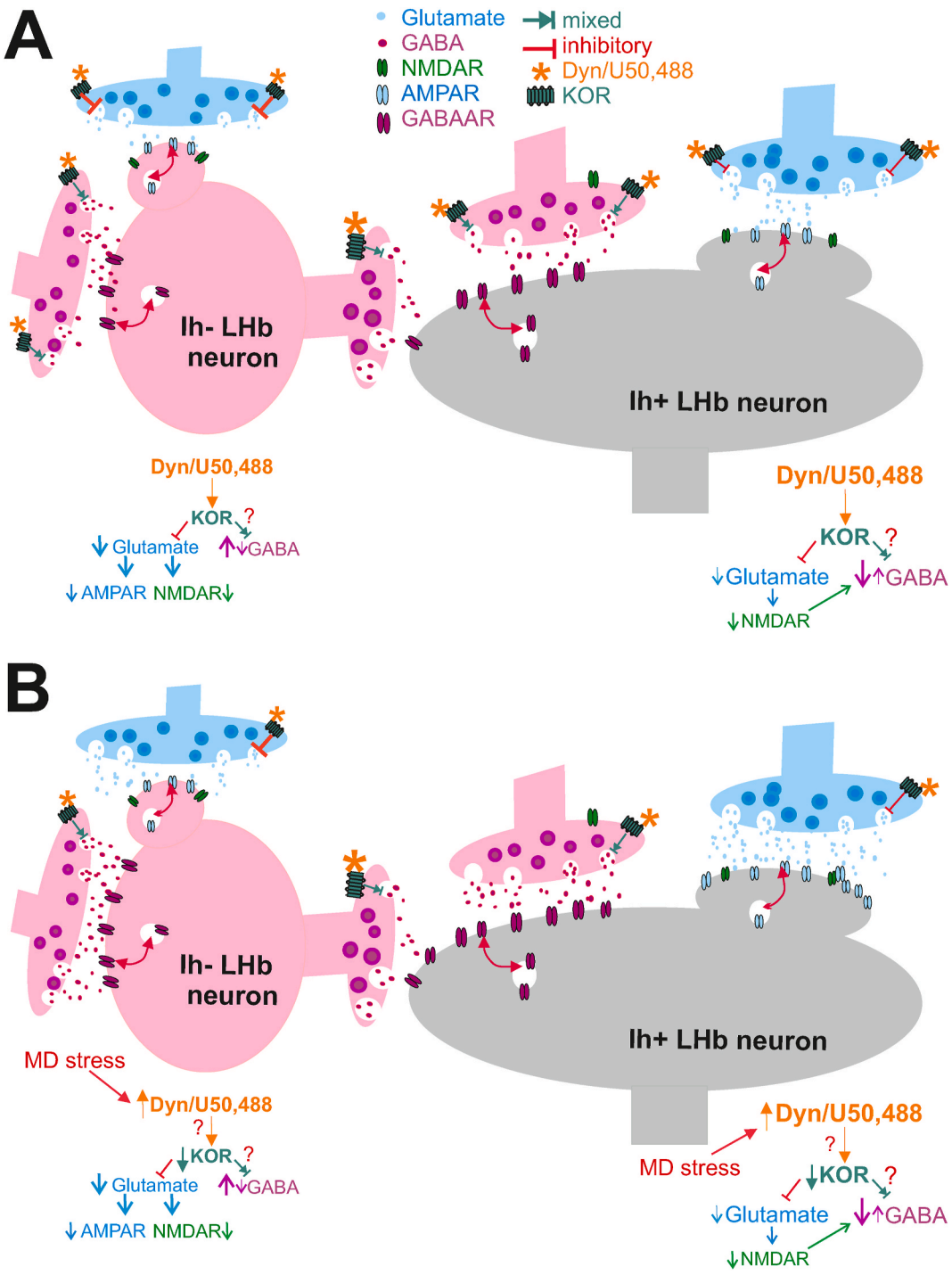

Fig. 9. Dyn/KOR dysregulation of LHb neuronal activity following MD. The figure depicts our proposed model of Dyn/KOR differential regulation of LHb neuronal excitability in Ih- and Ih+ LHb neurons in control un-stressed rats (A) and its loss following MD (B). Dyn/KOR stimulation uniformly and presynaptically suppresses glutamatergic transmission (glutamate release) in LHb neurons while its effects on GABA release can be either a decrease (predominant effect) or even an increase (in small subset of neurons). We hypothesize that the preferential reduction of presynaptic glutamate release by KOR stimulation that can equally decrease the post-synaptic excitatory function of AMPARs and NMDARs in Ih- neurons as well as a selective projection-specific KOR-induced increases in GABA release could contribute to KOR-induced reduction of Ih-neuronal excitability. On the other hand, KOR-induced reduction of presynaptic GABA release onto Ih+ neurons is the main determinant for the excitatory actions of KOR signaling in Ih+ neurons. We also hypothesize that GABA release onto Ih+ neurons may be potentiated by presynaptic and postsynaptic NMDAR activity where KOR-induced reduction of glutamate release and the subsequent reduced NMDAR activity could result in less release of GABA from presynaptic terminals onto Ih+ neurons. In this model, we favor the idea that Ih- neurons are GABAergic interneurons, therefore the inhibitory action of KOR on Ih- neurons in addition to excitatory effect of KOR stimulation on Ih+ neurons (glutamatergic projection neurons) will increase the excitatory output of LHb to downstream targets. We further hypothesize that MD stress engages Dyn/KOR signaling and upregulates this pathway with homeostatic decrease in KOR expression in response to Dyn hypertrophy. This loss of proper KOR signaling may contribute to MD-induced enhancement of presynaptic glutamate and GABA release onto LHb neurons although MD-induced postsynaptic potentiation of glutamatergic transmission could still facilitate the shift of E/I balance towards excitation in LHb neurons.

for activation of NMDARs for triggering NMDAR-dependent bursting of LHb neurons in originally silent or tonic neurons as previously shown (Yang et al., 2018a). However, it may seem contradictory when the blockade of NMDARs also promotes LHb bursting. RMP is an important factor in a voltage-dependent transition of firing mode in LHb neurons where hyperpolarization in spontaneously tonic-firing LHb neurons can switch their firing to bursting mode while depolarization of originally bursting LHb neurons can switch their firing to tonic-firing mode (Yang et al., 2018a). This is partly related to the activation of the pacemaker low-voltage-sensitive T-type Ca2+ channels (T-VSCC) that are inactivated at depolarized membrane potentials, but can be de-inactivated once membrane potential is hyperpolarized and they can then trigger T-VSCC-dependent burst firing of LHb neurons (Yang et al., 2018a). Therefore, it seems plausible that this switch of neuronal activity from silent or tonic to NMDAR- or T-VSCC-dependent bursting modes of firing during the blockade of $GABA_A$Rs or NMDARs, respectively, could partly mediate the decreases in the baseline activity of Ih- and specifically Ih+ LHb neurons. Interestingly, the high tonic activity of Ih+ LHb neurons was also abolished in the presence of both short-acting KOR antagonists (BTRX and aticaprant) where they both promoted bursting activity in current clamp recordings similar to the conditions with the blockade of NMDARs and $GABA_A$Rs suggesting that an endogenous Dyn-KOR tone may contribute to the maintenance of a higher basal tonic activity of Ih+ neurons. It is worth mentioning that although our experiments with both short-acting KOR antagonists (BTRX and aticaprant) validated that U50, 488 acts through KORs to alter LHb neuronal excitability, the significantly lower levels of neuronal excitability in the presence of BTRX in both Ih+ and Ih- neurons may suggest possible off-target effects of this compound on silencing LHb basal activity. Interestingly, while BTRX did not affect the spontaneous LHb neuronal activity and firing patterns in cell-attached recordings which were comparable to controls, aticaprant promoted tonic firing of LHb neurons that could be due to its MOR antagonistic properties as recently shown in VTA DA neurons (Margolis et al., 2020).

The effects of KOR signaling on each synaptic receptor seems to be sufficient to mediate the inhibitory effects of KOR signaling in Ih- neurons. On the other hand, in Ih+ neurons where an endogenous Dyn-KOR tone may maintain their higher tonic activity levels, either $GABA_A$Rs or NMDARs are sufficient to mediate KOR's stimulatory effects on their excitability. Our findings of KOR-induced suppression of presynaptic glutamatergic and GABAergic synaptic inputs to LHb neurons are consistent with previous studies of KOR activation in several brain regions including the hippocampus (Drake et al., 2007; Simmons and Chavkin, 1996), VTA (Ehrich et al., 2015; Ford et al., 2006, 2007; Margolis et al., 2003, 2005, 2006), bed nucleus of the stria terminalis (BNST) (Crowley et al., 2016; Li et al., 2012), NAc (Tejeda et al., 2017; Hjelmstad and Fields, 2003), central amygdala neurons (Gilpin et al., 2014; Kang-Park et al., 2015) and ventrolateral periaqueductal grey (Li and Kash, 2019). Although general findings in the literature indicate that presynaptic KOR activation, through Gi/Go G-protein-coupled signaling, inhibits neurotransmitter release, our observation of KOR-induced increases in GABA release in a small subset of LHb neurons also raises the possibility of a cell- and/or pathway-specific modulation of GABA terminals by presynaptic KORs. It is likely that differential expression of KORs on various presynaptic inputs projecting selectively to Ih+ or Ih- LHb neurons biases excitatory/inhibitory drive (E/I balance) that may favor increased/decreased LHb neuronal excitability, respectively, as shown in our model (Fig. 9). In fact, this model is supported by studies in the NAc wherein activation of presynaptic KORs decreases both excitatory and inhibitory synaptic drives onto NAc medium spiny neurons (MSNs), but the cell- and input-specific modification of E/I balance in MSNs by KORs preferentially results in decreases in excitatory drive of D1 MSNs and disinhibition of D2 MSNs (Tejeda et al., 2017). Therefore, we favor the idea that the preferential reduction of presynaptic glutamate release by KOR stimulation that can equally decrease the postsynaptic excitatory function of AMPARs and NMDARs in Ih- neurons as well as a selective projection-specific KOR-induced increase in GABA release (or maybe reduced inhibitory effect of KOR on GABA release due to KOR's restricted expression on these terminals) could contribute to the net KOR-induced reduction of Ih- neuronal excitability. On the other hand, the significant reduction of presynaptic GABA release in Ih+ neurons rather than reduced glutamate release may be the main determinant for the excitatory actions of KOR signaling in Ih+ neurons. It is also tempting to assume a scenario where GABA release can be potentiated by postsynaptic and presynaptic NMDAR activity (Xue et al., 2011; Nugent et al., 2007). In this case, postsynaptic NMDAR activation in Ih+ neurons can enhance GABA release through a retrograde signaling such as nitric oxide (NO) signaling and/through the action of presynaptic NMDARs in GABAergic terminals (those residing in GABAergic interneurons as well as presynaptic NMDARs on GABAergic terminals projecting to Ih+ LHb neurons). Therefore, KOR-induced reduction of glutamate release and the subsequent reduced postsynaptic/presynaptic NMDAR activity could also reduce the release of GABA from presynaptic terminals onto Ih+ neurons which could further augment the effects of KORs on presynaptic GABA release or be sufficient on its own to mediate KOR's effects as suggested by our data where we observed the loss of KOR's excitatory effects in Ih+ neurons with the blockade of NMDARs.

It should also be noted that in addition to synaptic regulation of Ih- and Ih+ LHb neuronal excitability at basal levels, there are inherent differences in membrane properties between Ih- and Ih+ neurons that were also subject to change by KOR stimulation. For example, we found that at baseline levels, Ih+ neurons have lower Rin than Ih- neurons possibly due to the basal larger conductance of HCN/Ih channels in these neurons compared to Ih- neurons as Ih is active at resting membrane potentials in LHb neurons (Good et al., 2013). U50,488 only increased Rin of Ih+ neurons suggesting that KOR stimulation may result in possible decreases in resting K+ conductance that underlie membrane resistance such as leak K+ channels (Ren, 2011) and their closure upon KOR stimulation could also promote the increased excitability of Ih+ LHb neurons. Irrespective of opposing effects on the excitability of Ih- and Ih+ neurons, stimulation of KOR lowered AP thresholds in both Ih- and Ih+ neurons. The excitatory effect of CRF is also associated with increases in Rin and lower AP thresholds (Authement et al., 2018), similar to our findings in Ih+ LHb neurons following KOR activation. Part of the change in Rin and AP threshold by CRF-CRFR1 signaling is related to its effects on the SK and BK K+ channels; which mediate mAHPs and fAHPs, respectively (Authement et al., 2018). These K+ channels play an important role in regulating AP frequency of LHb neurons in response to depolarization. We previously observed that CRF-CRFR1 signaling increases fAHPs (while reducing mAHPs) in LHb neurons, thereby inducing a more hyperpolarized inter-spike membrane potential which could prevent voltage-gated Na+ channel inactivation and thus support the high frequency firing of LHb neurons during prolonged depolarization (Authement et al., 2018). Here, KOR stimulation significantly increased fAHPs in only Ih+ LHb neurons. While at baseline levels, Ih- neurons had significantly larger mAHPs compared to Ih+ neurons (which could explain their lower neuronal excitability than Ih+ neurons), KOR stimulation decreased mAHPs in both neurons. This may seem contradictory for Ih- neurons, as any reduction in mAHPs should promote rather than decrease neuronal excitability, but hyperpolarization induced by KOR stimulation as indicated by KOR-induced lowering of AP threshold potentials in Ih- neurons could also suppress SK channel activation and result in reduced mAHPs while still preventing the cell from reaching AP threshold and spiking. On the other hand, the changes in fAHPs and mAHPs by KOR activation in Ih+ neurons resemble those following CRF which support high frequency firing. Altogether, these findings suggest that KOR activation may exert differential effects on LHb neuronal excitability through modulating resting and active ion conductance that drive the membrane potential towards negative voltages. It is important to note that the changes induced by KOR on intrinsic measurements were derived from AP

recordings with intact synaptic transmission which may not only be related to direct actions of KOR stimulation on LHb neurons, but also may involve KOR's indirect effects. This could be related to KOR modulation of fast synaptic transmission (e.g., through $GABA_ARs$, AMPARs, NMDARs) as well as a complex interactions with various neuromodulators through their G-coupled protein receptors (GPCRs). Examples include CRF-CRFR1, $GABA_BRs$, metabotropic glutamate receptors (mGluRs), D2 and D4 DA receptors, and 5HT receptors which have all been shown to regulate intrinsic properties and intrinsic excitability of LHb neurons (Authement et al., 2018; Yang et al., 2018a; Tchenio et al., 2017; Good et al., 2013; Root et al., 2015; Zuo et al., 2013, 2016; Jhou et al., 2013; Meye et al., 2013; Han et al., 2015). Altogether, the persistence/appearance of effects of KOR-stimulation on intrinsic membrane properties without a significant effect on neuronal excitability highlights the necessity of presynaptic KOR stimulation on synaptic transmission to drive KOR modulatory effects on LHb neuronal excitability rather than KOR-induced changes in intrinsic membrane properties of LHb neurons.

Previously, we also demonstrated that a single episode of MD at P9 as an established model of child neglect that is associated with depressive-like phenotype triggers an imbalance of glutamate/GABA signaling within the LHb which blunts the excitatory actions of CRF on LHb neurons (Shepard et al., 2018a; Authement et al., 2018). Therefore, we further tested the possibility of the involvement of Dyn/KOR signaling in LHb aberrant stress responsivity following MD. We confirmed that MD increased spontaneous LHb activity in both tonic and bursting modes, although the baseline excitability of Ih+ neurons were significantly lower than Ih+ neurons in non-MD rats with no such difference for Ih-neurons. Part of the absence of higher excitability of LHb neurons in Ih+ neurons of MD rats may also be explained by MD-induced promotion of LHb bursting as shown here. Note that in our previous study LHb neurons were not segregated based on Ih but consistently we did not detect differences between the excitability of LHb neurons in non-MD versus MD rats in intact synaptic transmission, while the intrinsic excitability (with blocked fast synaptic transmission) of LHb neurons were significantly higher in MD rats than those from non-MD rats due to downregulation of SK2 channels by MD which also mediates the insensitivity of LHb neuronal responses to CRF (Authement et al., 2018). Here, we also found that Ih- and Ih+ LHb neuronal responses to KOR stimulation were absent in MD rats. MD induced hypertrophy of Dyn resulting in homeostatic downregulation of presynaptic (and possibly postsynaptic) KORs within the LHb, therefore we speculate that while Dyn-A expression is upregulated in the LHb by MD, the downregulation of KOR expression could contribute to the blunted LHb neuronal responses to KOR activation in both Ih- and Ih+ neurons following MD. Although it is important to note that mRNA abundance does not equate to protein expression nor synaptic availability. Nevertheless, MD appears to dysregulate Dyn/KOR signaling at multiple levels that involve projections from Dyn-containing brain areas to the LHb as well as the KOR expression/availability on synaptic terminals within the LHb, consistent with earlier studies of ELS (Karkhanis et al., 2016; Pautassi et al., 2012; Nakamoto et al., 2020; Chang et al., 2019; Diaz et al., 2018; Lutz et al., 2018; Hays et al., 2012; Ploj and Nylander, 2003). Interestingly, MD potentiates both pre- and postsynaptic glutamatergic and GABAergic synapses onto LHb neurons although shifts E/I balance towards excitation in LHb neurons that supports the increased activity of LHb neurons (Authement et al., 2018). We hypothesize that MD-induced enhancement of presynaptic glutamate and GABA release onto LHb neurons may partly be the result of the loss of presynaptic KOR signaling in presynaptic terminals by MD although MD-induced postsynaptic potentiation of glutamatergic transmission triggered by decreases in SK channels could still facilitate the shift of E/I balance towards excitation. Whether these uniformed MD-induced synaptic adaptations are subject to change differentially by KOR signaling in Ih- and Ih+ neurons and subsequently alter cell- and projection-specific LHb pathways are open questions that merit further investigation. It would be worthwhile to test how the blockade of each synaptic component as well as the KOR antagonists affect spontaneous neuronal activity and firing patterns as well as neuronal and intrinsic excitability of Ih- and Ih+ LHb neurons with post-hoc identification of neurochemical nature of these neurons. In summary, we conclude that the impairment of proper cell-specific KOR-dependent fine tuning of LHb activity by MD could work in concert with MD-induced altered CRF signaling and partly contribute to dysregulated stress-responsivity within the LHb following this severe early life stress.

5. Conclusion and future directions

To our knowledge our study is the first to demonstrate the existence of the functional KOR signaling in the LHb that differentially affects the excitability of discrete subpopulations of LHb neurons, mainly through changes in synaptic transmission. We also provided evidence for dysregulation of Dyn/KOR signaling following MD, used as a model of ELS. Given that KORs play an important role in drug- and stress-induced synaptic plasticity (Tejeda and Bonci, 2019; Graziane et al., 2013; Polter et al., 2014), our future studies will focus on KOR modulation of MD-induced intrinsic and synaptic plasticity within the LHb and at specific synaptic inputs to the LHb that may contribute to the later development of reward dysregulation and psychopathology associated with this model. We will also explore the therapeutic potential of targeting of KORs within the LHb in the context of ELS-induced neuropsychiatric and substance use disorders.

CRediT authorship contribution statement

Sarah C. Simmons: Formal analysis, Data curation, Writing - original draft, Writing - review & editing. **Ryan D. Shepard:** Formal analysis, Data curation, Writing - review & editing. **Shawn Gouty:** Formal analysis, Data curation, Writing - review & editing. **Ludovic D. Langlois:** Formal analysis, Data curation, Writing - review & editing. **William J. Flerlage:** Writing - review & editing. **Brian M. Cox:** Writing - review & editing. **Fereshteh S. Nugent:** Formal analysis, Data curation, Writing - original draft, Writing - review & editing.

Declaration of competing interest

None.

Acknowledgements

The opinions and assertions contained herein are the private opinions of the authors and are not to be construed as official or reflecting the views of the Uniformed Services University of the Health Sciences or the Department of Defense or the Government of the United States. We are grateful to Drs. Irwin Lucki and Caroline Browne for their technical advice on qPCR experiments. The novel selective KOR antagonist (BTRX-084266) was generously provided by BlackThorn Therapeutics, Inc. We are especially thankful to Dr. Tanya Wallace from BlackThorn Therapeutics Inc. and Dr. Robert Koenig from the office of Technology Transfer at Henry M. Jackson Foundation for facilitating the Research Material Transfer of BTRX-084266.

Appendix A. Supplementary data

Supplementary data to this article can be found online at https://doi.org/10.1016/j.ynstr.2020.100267.

Funding

This work was supported by the National Institutes of Health (NIH)–National Institute of Drugs of Abuse (NIDA) Grant#R01 DA039533 to FSN. The funding agency did not contribute to writing this article or

deciding to submit it.

References

Abraham, A.D., et al., 2018. Kappa-opioid receptor activation in dopamine neurons disrupts behavioral inhibition. Neuropsychopharmacology 43 (2), 362–372.

Authement, M.E., et al., 2015. Histone deacetylase inhibition rescues maternal deprivation-induced GABAergic metaplasticity through restoration of AKAP signaling. Neuron 86 (5), 1240–1252.

Authement, M.E., et al., 2018. A role for corticotropin-releasing factor signaling in the lateral habenula and its modulation by early-life stress. Sci. Signal. 11 (520).

Berger, A.L., et al., 2018. The lateral habenula directs coping styles under conditions of stress via recruitment of the endocannabinoid system. Biol. Psychiatr. 84 (8), 611–623.

Bruchas, M.R., Chavkin, C., 2010. Kinase cascades and ligand-directed signaling at the kappa opioid receptor. Psychopharmacology (Berlin) 210 (2), 137–147.

Bruchas, M.R., Land, B.B., Chavkin, C., 2010. The dynorphin/kappa opioid system as a modulator of stress-induced and pro-addictive behaviors. Brain Res. 1314, 44–55.

Cahill, C.M., et al., 2014. Does the kappa opioid receptor system contribute to pain aversion? Front. Pharmacol. 5, 253.

Carr, G.V., et al., 2010. Antidepressant-like effects of kappa-opioid receptor antagonists in Wistar Kyoto rats. Neuropsychopharmacology 35 (3), 752–763.

Cerniauskas, I., et al., 2019. Chronic stress induces activity, synaptic, and transcriptional remodeling of the lateral habenula associated with deficits in motivated behaviors. Neuron 104 (5), 899–915 e8.

Chang, L., et al., 2019. Early life stress alters opioid receptor mRNA levels within the nucleus accumbens in a sex-dependent manner. Brain Res. 1710, 102–108.

Chapman, D.P., et al., 2004. Adverse childhood experiences and the risk of depressive disorders in adulthood. J. Affect. Disord. 82 (2), 217–225.

Chen, C., et al., 2020. Characterization of a Knockin mouse line expressing a fusion protein of kappa opioid receptor conjugated with tdTomato: 3-dimensional brain imaging via CLARITY. eNeuro 7 (4).

Code, R.A., Fallon, J.H., 1986. Some projections of dynorphin-immunoreactive neurons in the rat central nervous system. Neuropeptides 8 (2), 165–172.

Crowley, N.A., Kash, T.L., 2015. Kappa opioid receptor signaling in the brain: circuitry and implications for treatment. Prog. Neuro-Psychopharmacol. Biol. Psychiatry 62, 51–60.

Crowley, N.A., et al., 2016. Dynorphin controls the gain of an amygdalar anxiety circuit. Cell Rep 14 (12), 2774–2783.

Diaz, M.R., Przybysz, K.R., Rouzer, S.K., 2018. Age as a factor in stress and alcohol interactions: a critical role for the kappa opioid system. Alcohol 72, 9–18.

Drake, C.T., Chavkin, C., Milner, T.A., 2007. Opioid systems in the dentate gyrus. Prog. Brain Res. 163, 245–263.

Ehrich, J.M., et al., 2015. Kappa opioid receptor-induced aversion requires p38 MAPK activation in VTA dopamine neurons. J. Neurosci. 35 (37), 12917–12931.

Faturi, C.B., et al., 2010. Disruptions of the mother-infant relationship and stress-related behaviours: altered corticosterone secretion does not explain everything. Neurosci. Biobehav. Rev. 34 (6), 821–834.

Ford, C.P., Mark, G.P., Williams, J.T., 2006. Properties and opioid inhibition of mesolimbic dopamine neurons vary according to target location. J. Neurosci. 26 (10), 2788–2797.

Ford, C.P., Beckstead, M.J., Williams, J.T., 2007. Kappa opioid inhibition of somatodendritic dopamine inhibitory postsynaptic currents. J. Neurophysiol. 97 (1), 883–891.

Gilpin, N.W., et al., 2014. Kappa opioid receptor activation decreases inhibitory transmission and antagonizes alcohol effects in rat central amygdala. Neuropharmacology 77, 294–302.

Gomes, I., et al., 2020. Biased signaling by endogenous opioid peptides. Proc. Natl. Acad. Sci. Unit. States Am. 117 (21), 11820–11828.

Good, C.H., et al., 2013. Dopamine D4 receptor excitation of lateral habenula neurons via multiple cellular mechanisms. J. Neurosci. 33 (43), 16853–16864.

Graziane, N.M., et al., 2013. Kappa opioid receptors regulate stress-induced cocaine seeking and synaptic plasticity. Neuron 77 (5), 942–954.

Han, L.N., et al., 2015. Activation of serotonin(2C) receptors in the lateral habenular nucleus increases the expression of depression-related behaviors in the hemiparkinsonian rat. Neuropharmacology 93, 68–79.

Hays, S.L., et al., 2012. Long-term effects of neonatal stress on adult conditioned place preference (CPP) and hippocampal neurogenesis. Behav. Brain Res. 227 (1), 7–11.

Heim, C., Nemeroff, C.B., 2001. The role of childhood trauma in the neurobiology of mood and anxiety disorders: preclinical and clinical studies. Biol. Psychiatr. 49 (12), 1023–1039.

Hikosaka, O., 2010. The habenula: from stress evasion to value-based decision-making. Nat. Rev. Neurosci. 11 (7), 503–513.

Hjelmstad, G.O., Fields, H.L., 2003. Kappa opioid receptor activation in the nucleus accumbens inhibits glutamate and GABA release through different mechanisms. J. Neurophysiol. 89 (5), 2389–2395.

Hollt, V., 1986. Opioid peptide processing and receptor selectivity. Annu. Rev. Pharmacol. Toxicol. 26 (1), 59–77.

Hu, H., Cui, Y., Yang, Y., 2020. Circuits and functions of the lateral habenula in health and in disease. Nat. Rev. Neurosci. 21 (5), 277–295.

Jhou, T.C., et al., 2013. Cocaine drives aversive conditioning via delayed activation of dopamine-responsive habenular and midbrain pathways. J. Neurosci. 33 (17), 7501–7512.

Jones, C.M., Merrick, M.T., Houry, D.E., 2020. Identifying and preventing adverse childhood experiences: implications for clinical practice. J. Am. Med. Assoc. 323 (1), 25–26.

Kang-Park, M., et al., 2015. Interaction of CRF and kappa opioid systems on GABAergic neurotransmission in the mouse central amygdala. J. Pharmacol. Exp. Therapeut. 355 (2), 206–211.

Karkhanis, A.N., et al., 2016. Early-life social isolation stress increases kappa opioid receptor responsiveness and downregulates the dopamine system. Neuropsychopharmacology 41 (9), 2263–2274.

Land, B.B., et al., 2008. The dysphoric component of stress is encoded by activation of the dynorphin kappa-opioid system. J. Neurosci. 28 (2), 407–414.

Lecca, S., et al., 2020. Heterogeneous habenular neuronal ensembles during selection of defensive behaviors. Cell Rep 31 (10), 107752.

Li, C., Kash, T.L., 2019. κ-Opioid receptor modulation of GABAergic inputs onto ventrolateral periaqueductal gray dopamine neurons. Mol. Neuropsychiatr. 5 (4), 190–199.

Li, C., et al., 2012. Presynaptic inhibition of gamma-aminobutyric acid release in the bed nucleus of the stria terminalis by kappa opioid receptor signaling. Biol. Psychiatr. 71 (8), 725–732.

Llorente, R., et al., 2010. Sex-dependent maternal deprivation effects on brain monoamine content in adolescent rats. Neurosci. Lett. 479 (2), 112–117.

Lutz, P.E., et al., 2018. Epigenetic regulation of the kappa opioid receptor by child abuse. Biol. Psychiatr. 84 (10), 751–761.

Mansour, A., et al., 1987. Autoradiographic differentiation of mu, delta, and kappa opioid receptors in the rat forebrain and midbrain. J. Neurosci. 7 (8), 2445–2464.

Mantsch, J.R., et al., 2016. Stress-induced reinstatement of drug seeking: 20 Years of progress. Neuropsychopharmacology 41 (1), 335–356.

Margolis, E.B., Karkhanis, A.N., 2019. Dopaminergic cellular and circuit contributions to kappa opioid receptor mediated aversion. Neurochem. Int. 129, 104504.

Margolis, E.B., et al., 2003. Kappa-opioid agonists directly inhibit midbrain dopaminergic neurons. J. Neurosci. 23 (31), 9981–9986.

Margolis, E.B., et al., 2005. Both kappa and mu opioid agonists inhibit glutamatergic input to ventral tegmental area neurons. J. Neurophysiol. 93 (6), 3086–3093.

Margolis, E.B., et al., 2006. Kappa opioids selectively control dopaminergic neurons projecting to the prefrontal cortex. Proc. Natl. Acad. Sci. U. S. A. 103 (8), 2938–2942.

Margolis, E.B., et al., 2020. Differential effects of novel kappa opioid receptor antagonists on dopamine neurons using acute brain slice electrophysiology. bioRxiv 2020, 04.24.059352.

McLaughlin, J.P., Marton-Popovici, M., Chavkin, C., 2003. Kappa opioid receptor antagonism and prodynorphin gene disruption block stress-induced behavioral responses. J. Neurosci. 23 (13), 5674–5683.

Meye, F.J., et al., 2013. Synaptic and cellular profile of neurons in the lateral habenula. Front. Hum. Neurosci. 7, 860.

Nakamoto, K., Taniguchi, A., Tokuyama, S., 2020. Changes in opioid receptors, opioid peptides and morphine antinociception in mice subjected to early life stress. Eur. J. Pharmacol. 881, 173173.

Nugent, F.S., Penick, E.C., Kauer, J.A., 2007. Opioids block long-term potentiation of inhibitory synapses. Nature 446 (7139), 1086–1090.

Nuno-Perez, A., et al., 2018. Lateral habenula gone awry in depression: bridging cellular adaptations with therapeutics. Front. Neurosci. 12, 485.

Pautassi, R.M., et al., 2012. Early maternal separation affects ethanol-induced conditioning in a nor-BNI insensitive manner, but does not alter ethanol-induced locomotor activity. Pharmacol. Biochem. Behav. 100 (3), 630–638.

Ploj, K., Nylander, I., 2003. Long-term effects on brain opioid and opioid receptor like-1 receptors after short periods of maternal separation in rats. Neurosci. Lett. 345 (3), 195–197.

Poller, W.C., et al., 2011. Lateral habenular neurons projecting to reward-processing monoaminergic nuclei express hyperpolarization-activated cyclic nucleotid-gated cation channels. Neuroscience 193, 205–216.

Polter, A.M., et al., 2014. Poststress block of kappa opioid receptors rescues long-term potentiation of inhibitory synapses and prevents reinstatement of cocaine seeking. Biol. Psychiatr. 76 (10), 785–793.

Proulx, C.D., Hikosaka, O., Malinow, R., 2014. Reward processing by the lateral habenula in normal and depressive behaviors. Nat. Neurosci. 17 (9), 1146–1152.

Proulx, C.D., et al., 2018. A neural pathway controlling motivation to exert effort. Proc. Natl. Acad. Sci. U. S. A. 115 (22), 5792–5797.

Ren, D., 2011. Sodium leak channels in neuronal excitability and rhythmic behaviors. Neuron 72 (6), 899–911.

Root, D.H., et al., 2015. Norepinephrine activates dopamine D4 receptors in the rat lateral habenula. J. Neurosci. 35 (8), 3460–3469.

S.A.a.M.H.S. Administration, 2019. E., Substance Abuse and Mental Health Services Administration, Behavioral Health Barometer: United States, Volume 5: Indicators as Measured through the 2017 National Survey on Drug Use and Health and the National Survey of Substance Abuse Treatment Services. HHS Publication, Rockville, MD.

S.A.a.M.H.S. Administration, E., Center for Behavioral Health Statistics and Quality, 2017. National Survey on Drug Use and Health: Detailed Tables. Substance Abuse and Mental Health Services Administration. *Rockville, MD, 2018*.

Shepard, R.D., et al., 2018a. Ketamine reverses lateral habenula neuronal dysfunction and behavioral immobility in the forced swim test following maternal deprivation in late adolescent rats. Front. Synaptic Neurosci. 10, 39.

Shepard, R.D., et al., 2018b. Targeting histone deacetylation for recovery of maternal deprivation-induced changes in BDNF and AKAP150 expression in the VTA. Exp. Neurol. 309, 160–168.

Shepard, R.D., et al., 2020. Histone deacetylase inhibition reduces ventral tegmental area dopamine neuronal hyperexcitability involving AKAP150 signaling following maternal deprivation in juvenile male rats. J. Neurosci. Res. 98 (7), 1457–1467.
Simmons, M.L., Chavkin, C., 1996. Endogenous opioid regulation of hippocampal function. Int. Rev. Neurobiol. 39, 145–196.
Stamatakis, A.M., Stuber, G.D., 2012. Activation of lateral habenula inputs to the ventral midbrain promotes behavioral avoidance. Nat. Neurosci. 15 (8), 1105–1107.
Stamatakis, A.M., et al., 2016. Lateral hypothalamic area glutamatergic neurons and their projections to the lateral habenula regulate feeding and reward. J. Neurosci. 36 (2), 302–311.
Tchenio, A., et al., 2017. Limiting habenular hyperactivity ameliorates maternal separation-driven depressive-like symptoms. Nat. Commun. 8 (1), 1135.
Tejeda, H.A., Bonci, A., 2019. Dynorphin/kappa-opioid receptor control of dopamine dynamics: implications for negative affective states and psychiatric disorders. Brain Res. 1713, 91–101.
Tejeda, H.A., et al., 2017. Pathway- and cell-specific kappa-opioid receptor modulation of excitation-inhibition balance differentially gates D1 and D2 accumbens neuron activity. Neuron 93 (1), 147–163.
Thompson, M.P., Kingree, J.B., Lamis, D., 2019. Associations of adverse childhood experiences and suicidal behaviors in adulthood in a U.S. nationally representative sample. Child Care Health Dev. 45 (1), 121–128.
Van Bockstaele, E.J., Reyes, B.A., Valentino, R.J., 2010. The locus coeruleus: a key nucleus where stress and opioids intersect to mediate vulnerability to opiate abuse. Brain Res. 1314, 162–174.
Vincent, S.R., et al., 1982. Dynorphin-immunoreactive neurons in the central nervous system of the rat. Neurosci. Lett. 33 (2), 185–190.
Wagner, F., Weiss, T., Veh, R.W., 2017. Electrophysiological properties of neurons and synapses in the lateral habenular complex (LHb). Pharmacol. Biochem. Behav. 162, 38–45.
Wallace, M.L., et al., 2017. Genetically distinct parallel pathways in the entopeduncular nucleus for limbic and sensorimotor output of the basal ganglia. Neuron 94 (1), 138–152 e5.
Weber, E., Roth, K.A., Barchas, J.D., 1982a. Immunohistochemical distribution of alpha-neo-endorphin/dynorphin neuronal systems in rat brain: evidence for colocalization. Proc. Natl. Acad. Sci. U. S. A. 79 (9), 3062–3066.
Weber, E., Evans, C.J., Barchas, J.D., 1982b. Predominance of the amino-terminal octapeptide fragment of dynorphin in rat brain regions. Nature 299 (5878), 77–79.
Webster, J.F., et al., 2020. Disentangling neuronal inhibition and inhibitory pathways in the lateral habenula. Sci. Rep. 10 (1), 8490.
Weiss, T., Veh, R.W., 2011. Morphological and electrophysiological characteristics of neurons within identified subnuclei of the lateral habenula in rat brain slices. Neuroscience 172, 74–93.
Xue, J.G., et al., 2011. NMDA receptor activation enhances inhibitory GABAergic transmission onto hippocampal pyramidal neurons via presynaptic and postsynaptic mechanisms. J. Neurophysiol. 105 (6), 2897–2906.
Yang, Y., et al., 2018a. Ketamine blocks bursting in the lateral habenula to rapidly relieve depression. Nature 554 (7692), 317–322.
Yang, Y., et al., 2018b. Lateral habenula in the pathophysiology of depression. Curr. Opin. Neurobiol. 48, 90–96.
Zamir, N., Palkovits, M., Brownstein, M.J., 1984. Distribution of immunoreactive dynorphin A1-8 in discrete nuclei of the rat brain: comparison with dynorphin A. Brain Res 307 (1–2), 61–68.
Zhang, L., et al., 2016. Thirst is associated with suppression of habenula output and active stress coping: is there a role for a non-canonical vasopressin-glutamate pathway? Front. Neural Circ. 10, 13.
Zhang, L., et al., 2018. A GABAergic cell type in the lateral habenula links hypothalamic homeostatic and midbrain motivation circuits with sex steroid signaling. Transl. Psychiatry 8 (1), 50.
Zuo, W., et al., 2013. Cocaine facilitates glutamatergic transmission and activates lateral habenular neurons. Neuropharmacology 70, 180–189.
Zuo, W., et al., 2016. Serotonin stimulates lateral habenula via activation of the post-synaptic serotonin 2/3 receptors and transient receptor potential channels. Neuropharmacology 101, 449–459.